AIMS | African Institute for Mathematical Sciences CAMEROON

On the Multi-domain Bivariate Spectral Local Linearization Method for Systems of Non-similar Boundary Layer Differential Equations

Misile Kunene (misile.kunene@aims-cameroon.org)
African Institute for Mathematical Sciences (AIMS)
Cameroon

Supervised by: Dr. Vusi Mpendulo Magagula
University of Swaziland, Swaziland

18 May 2018

Submitted in Partial Fulfillment of a Structured Masters Degree at AIMS-Cameroon

Abstract

In this project, a novel approach for solving systems of non-similar boundary layer equations over a large time domain is presented. The method is called multi-domain bivariate spectral local linearization method (MD-BSLLM). This method makes use of Lagrange-Gauss-Lobbatto grid points, a linearization technique, and the spectral collocation method to approximate functions defined by bivariate Lagrange interpolation. The method is developed for a general system of n nonlinear partial differential equations. We demonstrate the application of the MD-BSLLM technique by solving a system of nonlinear partial differential equations that describes a class of non-similar boundary layer equations. Numerical experiments are conducted to show applicability and accuracy of the methods. Grid independence tests establish their accuracy, convergence and validity. The solution for the limiting case is used to validate their accuracy. This method is an extension of the work done by Motsa et al [25]. Motsa et al solved a system of nonlinear differential equations over a short value of the domain of ζ and in this case, we want to apply the same method over a large value of the domain of ζ . The approach of using spectral methods in both space and time have been successfully used by different researchers [23, 24], but however, most of them have done so in small domains of ζ . In this case, we extend the ideas presented by Motsa et al [25] to minimize computational resources. Ground breaking work on spectral methods were done by Canuto [13] and Trefethen [36].

Declaration

I, the undersigned, hereby declare that the work contained in this essay is my original work, and that any work done by others or by myself previously has been acknowledged and referenced accordingly.

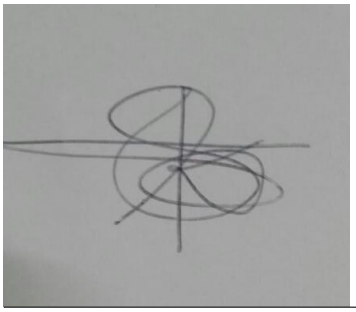

Misile Simisile Kunene, 18 May 2018.

Contents

1. Introduction

The important properties of the dynamics of non-Newtonian fluids which arise in engineering and science problems have been well researched and documented in the last decade. These properties have been modeled by non-linear partial differential equations (NPDEs). In Fluid Dynamics for example, the Burgers-Huxley equation is a prototype model that is normally used to describe interactions between reaction mechanisms, convection effects and diffusion transport [35]. Finding the solutions of these equations is very important in understanding the behavior of the problems. However, despite the success in modeling these processes, it remains difficult or impossible for researchers find the exact or explicit solutions of most of the model systems of differential equations [28]. Analytical methods to solve a limited number of nonlinear partial differential equations problems have been developed, some of which include the homotopy analysis method [1], the homotopy perturbation method [16] and the variational iteration method [15]. Thus, exact solutions for these problems are only limited to a small number of problems, hence there is a need to develop other methods such as numerical methods for solving the nonlinear partial differential equations (NPDE).

1.1 Literature Review

A number of numerical approaches have been developed to solve NPDEs, some of which have shown superior accuracy over others. In the recent years, researchers have developed numerous number of series solution methods that are used to solve non-linear non-similar boundary layer equations. These include the extended series solution [18] and the homotopy analysis method [32, 33]. The homotopy analysis method has been reported to be the most efficient series solution method and this is brought by the convergence control parameter which is incorporated into the homotopy equation. A comprehensive exposition of the underlying concepts and applications of the homotopy analysis method can be found in published books [20, 37]. One of the limitations of this method is that it is difficult to obtain completely analytical results since generating the incremental terms of the homotopy analysis method the series solution becomes cumbersome. Even though Motsa [24] presented a new variant of the homotopy analysis method, the bivariate spectral homotopy analysis method, the method still gives less accurate results when used to solve a large system of equations.

Finite difference methods have played a good role in solving boundary layer problems [26]. They have been successfully employed in other numerical methods with the intention to increase accuracy, such as the implicit Keller-box method [2]. The Keller-box method is one of the important techniques used to solve parabolic flow equations . Perot and Subramanian [31] analyzed the Keller-box scheme and generalized the method to arbitrary mesh grids. Their study revealed that the method is second order accurate on generic unstructured meshes and that the computational cost per solver iteration to obtain a desired accuracy is lower compared to finite volume schemes . Finite difference methods require a lot of grid points for increased accuracy, and this leads to high computational cost. To account for this, pseudo-spectral methods have been developed to solve boundary layer equations. They converge to the exact solution with few grid points and hence are computationally faster.

In 2014, Motsa et al [28] used the spectral relaxation method (SRM) and the spectral quasi-linearization method (SQLM) to solve highly non-linear partial differential equations that describes the unsteady heat transfer in a nano-fluid over a permeable stretching surface. The results they got were in line with those by Bachok et al [3]. Motsa et al showed that the SQLM converges faster than the SRM to the true

solution, the SRM is more accurate than the SQLM and also that the SQLM can resolve multiple solutions compared to the SRM. An explanation to the accuracy observation is that the SQLM solves the system of equations as coupled differentials. The system of equations are normally written in matrix form. Hence large system of equations imply very large matrix systems which are more liable to suffer from ill-conditions leading to inaccurate results due to round-off errors.

The quest for the most optimal method of solving nonlinear problems in fluid dynamics is what drives the ever growing interests in the development of new methods and the modifications and improvement of the existing analytical and numerical methods. Magagula et al [21] developed the bivariate interpolated spectral quasi-linearization method (BI-SQLM) and assessed its accuracy, robustness and effectiveness in solving non-linear partial differential equations. Numerical simulations were conducted on the KdV-Burgers equation, the Fisher equation, Burgers-Fisher equation, Fitzhugh-Nagumo equation and also the Burgers-Huxley equation. Their results revealed that this method is uniformly accurate and valid over large intervals of space and time domain [24].

As a way of addressing the aforementioned numerical difficulties such as accuracy and computational costs, Motsa et al [27] proposed a highly accurate and convergent iterative algorithm for non-linear systems of equations that model boundary layer flow problems. This method is called the spectral local linearization method (SLLM). Their results reveal that the SLLM performs better than any other numerical method in terms of accuracy, simplicity and also efficiency in a small domain. This was in line with what Olamuyiwa [29] discovered when he solved the equations that modeled the unsteady free convective heat and mass transfer on a stretching surface in a porous medium using the SRM, SQLM and also the SLLM. One of the limitations of the SLLM is that it is only reliable when solving systems of equations in a small domain. At very large domains, the accuracy of the method is being reduced.

In this essay, we modify the SLLM and solve a nonlinear system of partial differential equations in a large domain. The domain is broken down into small subinterval and the systems of partial differential equations is solved in each of the subintervals. The new method is called the multi-domain bivariate spectral local linearzation method (MD-BSLLM). In chapter 2, we provide a mathematical formulation of the MD-BSLLM.

1.2 Preliminaries and Prerequisites

In this section, we begin with by stating some important definitions, theorems and elementary theory that will be constantly used throughout this work.

1.2.1 Definition. Let $f : U \to \mathbb{R}$ and $F : \mathbb{R}^{n^k} \times \mathbb{R}^{n^{k-1}} \times \cdots \times \mathbb{R}^n \times \mathbb{R} \times U \to \mathbb{R}$ be mappings , where $k \geq 1$. Then the expression of the form:

$$F(D^k u(x), D^{k-1}u(x), ..., Du(x), u(x), x) = 0, \quad (x \in U) \tag{1.2.1}$$

is called the k^{th} order partial differential equation with u the unknown [11].

1.2.2 Definition. The partial differential equation (1.2.1) is called linear if it has the form:

$$\sum_{|\alpha| \leq k} a_\alpha(x) D^\alpha u = f(x) \tag{1.2.2}$$

for given functions $a_\alpha \quad (|\alpha \leq k|)$ and f. If $f = 0$, then the linear partial differential equation is called homogeneous, otherwise non-homogeneous [11].

1.2.3 Definition. The partial differential equation (1.2.1) is said to be semi-linear if it has the form:

$$\sum_{|\alpha|=k} a_\alpha(x)(D^\alpha u + a_0(D^{k-1})u, ..., Du, u, x) = 0. \tag{1.2.3}$$

[11]

1.2.4 Definition. The partial differential equation (1.2.1) is said to be quasilinear if it has the form:

$$\sum_{|\alpha|=k} a_\alpha(x)(D^{k-1}u, ..., Du, u, x)D^\alpha u + a_0(D^{k-1}u, ..., Du, u, x) = 0. \tag{1.2.4}$$

[11]

1.2.5 Definition. The partial differential equation (1.2.1) is said to be fully non-linear if it depends nonlinearly upon the highest order derivatives [11].

1.2.6 Definition. An expression of the form:

$$\mathbf{F}(D^k\mathbf{u}(x), D^{k-1}\mathbf{u}(x), ..., D\mathbf{u}(x), \mathbf{u}(x), x) = 0, \quad (x \in U) \tag{1.2.5}$$

is called a k^{th}-order system of partial differential equations, where

$$\mathbf{F} : \mathbb{R}^{mn^k} \times \mathbb{R}^{mn^{k-1}} \times \cdots \times \mathbb{R}^{mn} \times \mathbb{R}^m \times \mathbb{R} \times U \to \mathbb{R}^m$$

is given and

$$\mathbf{u} : U \to \mathbb{R}^m, \quad \mathbf{u} = (u^1, \cdots, u^m)$$

is the unknown [11].

In numerical approximation, we characterize the applicability of a numerical method in solving PDE by its stability, consistency and convergence [26].

1.2.7 Definition. A one-step difference method with a local truncation error $\tau_i(h)$ is said to be consistent with the differential equation it approximates if

$$\lim_{h\to 0} \max_{1\le i\le N} |\tau_i(h)| = 0, \tag{1.2.6}$$

where the local truncation error at a specified step measures the amount by which the exact solution to the differential equation fails to satisfy the difference equation being used for the approximation at that step [4].

1.2.8 Definition. A one-step difference method is said to be convergent if

$$\lim_{h\to 0} \max_{1\le i\le N} |f_i - f(t_i)| = 0, \tag{1.2.7}$$

where $f(t_i)$ is the exact solution and f_i is the approximation obtained from the difference method [4].

1.2.9 Definition. A numerical method is said to be stable if small changes in the initial conditions or data produce correspondingly small changes in the subsequent approximations [26].

1.2.10 Definition. Let A and P be two points in space. A stream function $\varphi(x, y, t)$ in the point P with two dimensional coordinates (x, y) and as a function of time t for a fluid flow is defined as

$$\varphi(x, y, t) = \int_A^P (udy - vdx) \tag{1.2.8}$$

[5].

1.2.11 Definition. The Taylor series of a real or complex valued function $f(x)$ that is infinitely differentiable at a real or complex number a is the power series given by

$$f(x) \approx f(a) + (x-a)f'(a) + \frac{(x-a)^2}{2!}f''(a) + \frac{(x-a)^3}{3!}f'''(x) + \cdots [12]. \tag{1.2.9}$$

1.2.12 Definition. Let f_a be the approximation of the solution f of the equation $F(f)(x) = g(x)$. Then the residual is defined to be the maximum of the norm of the difference

$$\max_{x \in \chi} |g(x) - F(f_a)(x)| \tag{1.2.10}$$

over the domain χ [12].

1.2.13 Definition. The set of points given by

$$x_p = -\cos\left(p\frac{\pi}{N}\right) \quad \text{for} \quad p = 0, 1, \cdots, N, \quad N \in \mathbb{N} \tag{1.2.11}$$

are referred to as Chebyshev-Gauss-Lobatto points [14].

1.2.14 Definition. We define the Grashof number (Gr) as a dimensionless number which arises in fluid dynamics and heat transfer which approximates the ratio of the upward force exerted by a fluid that opposes the weight of an immersed object to the vicious force acting on a fluid [34].

1.2.15 Definition. In heat transfer at the surface within a fluid, we refer to the Nusselt number (Nu) as the ratio of convective and conductive heat transfers across the boundary [7].

1.2.16 Definition. We define the Prandtl number (Pr) as a dimensionless number that approximates the ratio of momentum diffusivity to thermal diffusivity [9].

1.2.17 Definition. The Sherwood number (Sh) is defined as a dimensionless number used in mass transfer operations which represents the ratio of the convective flow to the rate of diffusive mass transport [30].

1.2.18 Gauss-Seidel Method. This is an iterative technique that is used to solve a square system of n linear equations [12] presented in the form:

$$A\mathbf{x} = \mathbf{b}. \tag{1.2.12}$$

It is defined by the iteration

$$L_*\mathbf{x}^{(k+1)} = \mathbf{b} - U\mathbf{x}^{(k)}, \tag{1.2.13}$$

where $\mathbf{x}^{(k)}$ is the k^{th} approximation of $\mathbf{x}$, $\mathbf{x}^{(k+1)}$ is the next or $(k+1)$ iterations of $\mathbf{x}$ and the matrix A is decomposed into a lower triangular component L_* and a strictly upper triangular component $U : A = L_* + U$. The solution at the current iteration is given by

$$\mathbf{x}^{(k+1)} = L_*^{-1}(\mathbf{b} - U\mathbf{x}^{(k)}). \tag{1.2.14}$$

. The components of $\mathbf{x}^{(k+1)}$ are given by

$$x_i^{(k+1)} = \frac{1}{a_{ii}} \left(b_i - \sum_{j=1}^{i-1} a_{i,j} x_j^{(k+1)} - \sum_{j=i+1}^{n} a_{i,j} x_j^{(k)} \right), \quad 1, 2, \cdots, n. \tag{1.2.15}$$

The values of $\mathbf{x}^{(k+1)}$ are computed until the difference between the previous solution and the current solution is sufficiently a very small residual.

1.2.19 Dominant Balance Method. Let

$$\sum_{|\alpha| \leq k} a_\alpha(x) D^\alpha u = f(x) \tag{1.2.16}$$

be a nonlinear differential equation. Then the method of dominant balance [6] involves looking for a local solution of (1.2.16) of the form $u = e^{S(x)}$ as $x \to x_0$. The solution u is then substituted into the equation (1.2.16) and the dominant terms are retained. The resultant equation is then solved asymptotically for the value of $S(x)$. We continue like this until the full leading behavior is obtained. The consistency of the made assumptions is checked.

2. Mathematical Formulation of the MD-BSLLM

In this chapter, we present to the reader a mathematical formulation of the MD-BSLLM. We first give a brief overview of the spectral collocation method in section 2.1 and then later generalize the MD-BSLLM in section 2.2.

2.1 Spectral Collocation Method for Nonlinear PDE

Given a set of discrete experimental data $(x_0, f_0), (x_1, f_1), \cdots, (x_n, f_n)$, we want to find a function u such that $u(x_i) = f_i$ for all $i = 0, 1, \cdots, n$. The process of finding such a polynomial is termed interpolation. The points $x_0, x_1, \cdots, x_n$ are called nodes [12]. The process of finding a polynomial that passes through a given data set is called polynomial interpolation.

The following theorem has been taken from Davis et al [10].

2.1.1 Theorem. *(Existence and uniqueness theorem for polynomial interpolation) Given any $n+1$ distinct points (real or complex) $x_0, x_1, \cdots, x_n \quad (x_i \neq x_j)$ with associated values $f_0, f_1, \cdots, f_n$ (real or complex), there exist a unique polynomial $P_n(x)$ of degree of at most n, for which*

$$P_n(x_i) = f_i \quad \forall i \in \{0, 1, \cdots, n\}. \tag{2.1.1}$$

Proof. By definition, a polynomial of degree at most n over a field $\mathbb{C}$ is of the form:

$$P_n(x) = a_0 + a_1 x + \cdots + a_n x^n, \quad a_i \in \mathbb{C} \quad \forall \quad i = 0, 1, \cdots, n. \tag{2.1.2}$$

Then $P_n(x_i) = f_i$ if and only if

$$a_0 + a_1 x_i + \cdots + a_n x_i^n = f_i, \quad \forall i = 0, 1, \cdots, n. \tag{2.1.3}$$

Evaluating (2.1.3) for all $i = 0, 1, \cdots, n$ we obtain the following system

$$\begin{aligned} a_0 + a_1 x_0 + \cdots + a_n x_0^n &= f_0 \\ a_0 + a_1 x_1 + \cdots + a_n x_1^n &= f_1 \\ &\vdots \\ a_0 + a_1 x_n + \cdots + a_n x_n^n &= f_n, \end{aligned}$$

which can be written in matrix form:

$$\begin{bmatrix} 1 & x_0 & \cdots & x_0^n \\ 1 & x_1 & \cdots & x_1^n \\ & & \vdots & \\ 1 & x_n & \cdots & x_n^n \end{bmatrix} \begin{bmatrix} a_0 \\ a_1 \\ \vdots \\ a_n \end{bmatrix} = \begin{bmatrix} f_0 \\ f_1 \\ \vdots \\ f_n \end{bmatrix}. \tag{2.1.4}$$

Let

$$A = \begin{vmatrix} 1 & x_0 & \cdots & x_0^n \\ 1 & x_1 & \cdots & x_1^n \\ & & \vdots & \\ 1 & x_n & \cdots & x_n^n \end{vmatrix}.$$

The matrix system in (2.1.4) has a unique solution if and only if A is non-singular, hence we investigate the determinant of A. The determinant of A is called the Vandermonde determinant and it is denoted by:

$$V(x_0, x_1, \cdots, x_n) = \begin{vmatrix} 1 & x_0 & \cdots & x_0^n \\ 1 & x_1 & \cdots & x_1^n \\ & & \vdots & \\ 1 & x_n & \cdots & x_n^n \end{vmatrix}. \tag{2.1.5}$$

We define

$$Q(x) = V(x_0, x_1, \cdots, x_{n-1}, x) = \begin{vmatrix} 1 & x_0 & \cdots & x_0^n \\ 1 & x_1 & \cdots & x_1^n \\ & & \vdots & \\ 1 & x & \cdots & x^n \end{vmatrix}, \tag{2.1.6}$$

then evaluating $Q(x)$ with respect to the last row we obtain a polynomial of degree at most n in the variable x. Note that $Q(x_i) = 0 \quad \forall i = 0, 1, 2, \cdots, n$ since for each i, the $i^{th} + 1$ row and the last row will be identical. We can clearly see that $Q(x)$ is a polynomial of degree n with n zeros, namely $x_0, x_1, \cdots, x_{n-1}$. We write $Q(x)$ in the form:

$$Q(x) = k(x - x_0)(x - x_1)\cdots(x - x_{n-1}), \tag{2.1.7}$$

where k is the coefficient of x^n (minor of x^n). Computing the minor carefully we have:

$$k = V(x_0, x_1, \cdots, x_{n-1}),$$

and (2.1.7) become

$$Q(x) = V(x_0, x_1, \cdots, x_{n-1}) \prod_{i=0}^{n-1} (x - x_i). \tag{2.1.8}$$

It follows that

$$V(x_0, x_1, \cdots, x_n) = Q(x_n) = Q(x) = V(x_0, x_1, \cdots, x_{n-1}) \prod_{i=0}^{n-1} (x - x_i), \tag{2.1.9}$$

and by substituting n by $n-1, n-2, \cdots, 2, 1$, we have:

$$\begin{aligned} V(x_0, x_1, x_2, \cdots, x_{n-2}, x_{n-1}) &= V(x_0, x_1, x_2, \cdots, x_{n-3}, x_{n-2}) \prod_{i=0}^{n-2} (x_n - x_i), \\ V(x_0, x_1, x_2, \cdots, x_{n-3}, x_{n-2}) &= V(x_0, x_1, x_2, \cdots, x_{n-4}, x_{n-3}) \prod_{i=0}^{n-3} (x_n - x_i), \\ &\vdots \\ V(x_0, x_1) &= V(x_0)(x_1 - x_0), \\ V(x_0) &= 1. \end{aligned}$$

It follows by recursion that

$$\begin{aligned} V(x_0, x_1, x_n) &= (x_1 - x_0) \left(\prod_{i=0}^{1} (x_2 - x_i) \right) \cdots \left(\prod_{i=0}^{n-1} (x_n - x_i) \right), \\ &= \prod_{1 \le j < i \le n} (x_i - x_j) \neq 0 \quad \text{since} \quad x_i \neq x_j \quad \forall i \neq j. \end{aligned}$$

Hence (2.1.3) has a unique solution, which is what we wanted to show. □

2.1.2 Theorem. *(Weierstruss Approximation Theorem [12]) Let f be defined and continuous on the interval $[a, b]$. Then for any $\epsilon > 0$ given, there exist a sequence of polynomials (P_n), defined on $[a, b]$ with the property that*

$$|f(x) - P_n(x)| < \epsilon \quad \forall x \in [a, b]. \tag{2.1.10}$$

The above theorem asserts the possibility of uniform approximation by polynomials to continuous functions over a closed interval.

2.1.3 Definition. (Lagrange interpolating polynomial [12]) Given a set of $n+1$ data points $(x_0, f_0), (x_1, f_1), \cdots, (x_n, f_n)$ where no two x_k for $k = 0, 1, \cdots, n$ are the same, we define the Lagrange interpolating polynomial as a linear combination

$$P_n(x) := \sum_{i=0}^{n} f_i L_i(x) \tag{2.1.11}$$

of Lagrange basis polynomial

$$L_i(x) = \prod_{k=0, i\neq k}^{n} \frac{(x - x_k)}{(x_i - x_k)}, \tag{2.1.12}$$

with $L_i(x_k) = \begin{cases} 0, & \text{if} \quad i \neq k \\ 1, & \text{otherwise.} \end{cases}$

2.2 The Multi-domain Bivariate Spectral Local Linearization Method

In this section, we are going to generalize the multi-domain bivariate spectral local linearization method (MD-BSLLM) that is used to solve non-linear PDE. We consider a system of n non-linear PDE

$$\begin{aligned} \Gamma_1(H_1, H_2, \cdots, H_n) &= 0 \\ \Gamma_2(H_1, H_2, \cdots, H_n) &= 0 \\ &\vdots \\ \Gamma_n(H_1, H_2, \cdots, H_n) &= 0 \end{aligned} \tag{2.2.1}$$

where:

$$H_k = \left(f_k, \frac{\partial f_k}{\partial \eta}, ..., \frac{\partial f_k^{(p)}}{\partial \eta}, \frac{\partial f_k}{\partial \zeta}, \frac{\partial}{\partial \zeta}\left(\frac{\partial f_k}{\partial \eta}\right) \right) \quad \text{for} \quad k = 1, 2, .., n,$$

Γ_k for $k = 1, 2, .., n$ are non-linear operators containing all the spatial derivatives of $f_k(\eta, \zeta)$, p is the order of differentiation and $(\eta, \zeta) \in [-1, 1] \times [-1, 1]$. We assume that the solution can be approximated by the bivariate Lagrange interpolating polynomial of the form:

$$f(\eta, \zeta) = \sum_{i=0}^{N_\eta} \sum_{j=0}^{N_\zeta} f_k(\eta, \zeta) L_i(\eta) L_j(\zeta), \quad k = 1, 2, \cdots, n, \tag{2.2.2}$$

where $N_\eta + 1$ and $N_\zeta + 1$ are the number of interpolating points in the η and in the ζ directions respectively, L_i and L_j are the cardinal Lagrange polynomials. The points

$$\{\eta_i\} = \left\{\cos\left(\frac{\pi i}{N_\eta}\right)\right\}_{i=0}^{N_\eta}, \quad \{\zeta_j\} = \left\{\cos\left(\frac{\pi j}{N_\zeta}\right)\right\}_{j=0}^{N_\zeta}$$

are the Chebyshev-Gauss-Lobatto grid points. We first linearize the k^{th} equation in (2.2.1) by applying the local linearizaion technique. To do so, we assume that the difference between the current $(r+1)$ and the previous solution (r) is small enough so that by the Taylor series expansion, we have:

$$\Gamma_k(H_{1,r+1}, H_{2,r+1}, \cdots, H_{n,r+1}) \approx \Gamma_k(H_{1,r}, H_{2,r}, \cdots, H_{n,r}) + \nabla_{f_k}\Gamma_k(H_{1,r}, H_{2,r}, \cdots, H_{n,r}) \cdot [H_{k,r+1} - H_{k,r}], \tag{2.2.3}$$

where

$$\nabla_{f_k} = \left(\frac{\partial}{\partial f_k}, \frac{\partial}{\partial f_k'}, \cdots, \frac{\partial}{\partial f_k^{(p)}}, \frac{\partial}{\partial\left(\frac{\partial f_k}{\partial\zeta}\right)}, \frac{\partial}{\partial\left(\frac{f_k'}{\partial\zeta}\right)}\right) \quad \text{for} \quad k = 1, 2, \cdots, n.$$

For $k = 1$, we can expand (2.2.3) as follows:

$$\begin{aligned}
\Gamma_1(H_{1,r+1}, H_{2,r+1}, \cdots, H_{n,r+1}) &\approx \Gamma_1 + \nabla_{f_1}\Gamma_1 \cdot [H_{1,r+1} - H_{1,r}] \\
&= \Gamma_1 + \left(\frac{\partial}{\partial f_1}, \frac{\partial}{\partial f_1'}, \cdots, \frac{\partial}{\partial f_1^{(p)}}, \frac{\partial}{\partial\left(\frac{\partial f_1}{\partial\zeta}\right)}, \frac{\partial}{\partial\left(\frac{f_1'}{\partial\zeta}\right)}\right)\Gamma_1 \cdot [H_{1,r+1} - H_{1,r}] \\
&= \Gamma_1 + [H_{1,r+1} - H_{1,r}] \cdot \left(\frac{\partial\Gamma}{\partial f_1}, \frac{\partial\Gamma_1}{\partial f_1'}, \cdots, \frac{\partial\Gamma_1}{\partial f_1^{(p)}}, \frac{\partial\Gamma_1}{\partial\left(\frac{\partial f_1}{\partial\zeta}\right)}, \frac{\partial\Gamma_1}{\partial\left(\frac{f_1'}{\partial\zeta}\right)}\right)
\end{aligned}$$

where $\Gamma_1 = \Gamma_1(H_{1,r}, H_{2,r}, \cdots, H_{n,r})$ and p is the order of differentiation. Substituting the above approximation into the first equation in (2.2.3) we have:

$$\begin{aligned}
H_{1,r+1} \cdot \left(\frac{\partial\Gamma_1}{\partial f_1}, \frac{\partial\Gamma_1}{\partial f_1'}, \cdots, \frac{\partial\Gamma_1}{\partial f_1^{(p)}}, \frac{\partial\Gamma_1}{\partial\left(\frac{\partial f_1}{\partial\zeta}\right)}, \frac{\partial\Gamma_1}{\partial\left(\frac{f_1'}{\partial\zeta}\right)}\right) = & H_{1,r} \cdot \left(\frac{\partial\Gamma_1}{\partial f_1}, \frac{\partial\Gamma_1}{\partial f_1'}, \cdots, \frac{\partial\Gamma_1}{\partial f_1^{(p)}}, \frac{\partial\Gamma_1}{\partial\left(\frac{\partial f_1}{\partial\zeta}\right)}, \frac{\partial\Gamma_1}{\partial\left(\frac{f_1'}{\partial\zeta}\right)}\right) \\
& - \Gamma_1
\end{aligned}$$

or

$$\left(\sum_{s=0}^{p}\frac{\partial\Gamma_1}{\partial f_{1,r}^{(s)}}f_{1,r+1}^{(s)} + \frac{\partial\Gamma_1}{\partial(\frac{\partial f_{1,r}}{\partial\zeta})}\frac{\partial f_{1,r+1}}{\partial\zeta} + \frac{\partial\Gamma_1}{\partial(\frac{\partial f_{1,r}'}{\partial\zeta})}\frac{\partial f_{1,r}'}{\partial\zeta}\right) = \sum_{s=0}^{p}\frac{\partial\Gamma_1}{\partial f_{1,r}^{(s)}}f_{1,r}^{(s)} + \frac{\partial\Gamma_1}{\partial(\frac{\partial f_{1,r}}{\partial\zeta})}\frac{\partial f_{1,r}}{\partial\zeta} + \frac{\partial\Gamma_1}{\partial(\frac{\partial f_{1,r}'}{\partial\zeta})}\frac{\partial f_{1,r}'}{\partial\zeta} - \Gamma_1$$

A similar computation is carried out for $k = 2, \cdots, n$. The resultant system of n linear equations is of

the form

$$\begin{aligned}
&\sum_{s=0}^{p} \alpha_{s,r}^{(1)}(\eta,\zeta) f_{1,r+1}^{(s)} + \beta_r^{(1)}(\eta,\zeta)\frac{\partial f_{1,r+1}}{\partial \zeta} + \gamma_r^{(1)}(\eta,\zeta)\frac{\partial f'_{1,r+1}}{\partial \zeta} = R_1(\eta,\zeta)\\
&\sum_{s=0}^{p} \alpha_{s,r}^{(2)}(\eta,\zeta) f_{2,r+1}^{(s)} + \beta_r^{(2)}(\eta,\zeta)\frac{\partial f_{2,r+1}}{\partial \zeta} + \gamma_r^{(2)}(\eta,\zeta)\frac{\partial f'_{2,r+1}}{\partial \zeta} = R_2(\eta,\zeta)\\
&\qquad\qquad\vdots\\
&\sum_{s=0}^{p} \alpha_{s,r}^{(n)}(\eta,\zeta) f_{n,r+1}^{(s)} + \beta_r^{(n)}(\eta,\zeta)\frac{\partial f_{n,r+1}}{\partial \zeta} + \gamma_r^{(n)}(\eta,\zeta)\frac{\partial f'_{2,r+1}}{\partial \zeta} = R_n(\eta,\zeta),
\end{aligned} \tag{2.2.4}$$

where $\alpha_{s,r}^{(k)}(\eta,\zeta), \beta_r^{(k)}(\eta,\zeta), \gamma_r^{(k)}(\eta,\zeta)$ are variable coefficients of $f_{k,r+1}^{(s)}(\eta,\zeta), \frac{\partial f_{k,r+1}}{\partial \zeta}, \frac{\partial f'_{k,r+1}}{\partial \zeta}$ respectively, for $k = 1, 2, ..., n$ and $s = 0, 1, .., p$. To find the values of the variable coefficients, we use the following formulas:

$$\alpha_{s,r}^{(k)}(\eta,\zeta) = \frac{\partial \Gamma_k}{\partial f_{k,r}^{(s)}}, \tag{2.2.5}$$

$$\beta_r^{(k)}(\eta,\zeta) = \frac{\partial \Gamma_k}{\partial(\frac{\partial f_{k,r}}{\partial \zeta})}, \tag{2.2.6}$$

$$\gamma_r^{(k)}(\eta,\zeta) = \frac{\partial \Gamma_k}{\partial(\frac{\partial f'_{k,r}}{\partial \zeta})}. \tag{2.2.7}$$

The k^{th} right hand side is generally given by:

$$R_k(\eta,\zeta) = \sum_{s=0}^{p} \frac{\partial \Gamma_1}{\partial f_{k,r}^{(s)}} f_{k,r}^{(s)} + \frac{\partial \Gamma_1}{\partial(\frac{\partial f_{k,r}}{\partial \zeta})}\frac{\partial f_{k,r}}{\partial \zeta} + \frac{\partial \Gamma_1}{\partial(\frac{\partial f'_{k,r}}{\partial \zeta})}\frac{\partial f'_{k,r}}{\partial \zeta} - \Gamma_1 \quad \text{for} \quad k = 1, 2, \cdots, n. \tag{2.2.8}$$

To obtain a decoupled iteration scheme, we appeal to the Gauss-Seidel [27] approach of decoupling linear algebraic systems in linear algebra applications. We therefore arrange the equations in a particular order and solve them in a chronological order. Starting from an initial guess of $\Gamma_{1,0}, \Gamma_{2,0}, \cdots, \Gamma_{n,0}$, we find the solution of Γ_i in the current iteration level $\Gamma_{i,r+1}$ by using the updated values of $\Gamma_m, \quad (m < i)$. To solve the iteration scheme in (2.2.4), we require the interval in which the governing equations are defined to be $[-1, 1]$ [14], hence we transform the space working interval $[a, b]$ and the time working interval $[0, T]$ of the governing equations into $[-1, 1]$ by the linear mappings

$$\eta = \frac{(b-a)(x+1)}{2} \quad \text{and} \quad \zeta = \frac{T(t+1)}{2} \tag{2.2.9}$$

respectively. Moreover, we also decompose the interval $[0, T]$ into q non-overlapping sub-intervals $I_l = [\zeta_{l-1}, \zeta_l]$ for $l = 1, 2, \cdots, q$. The system of equations is then solved in each of these subintervals, at the Chebyshev Gauss-Lobatto points. We denote the solutions in each subinterval I_l by $f_k^{(l)}(\eta,\zeta)$ for $k = 1, 2, \cdots, n$ and $l = 1, 2, \cdots, q$. In the first sub-interval I_1, the solutions $f_k^{(1)}(\zeta,\eta)$ for $k = 1, 2, \cdots, n$ are solved subject to the initial condition $f_k^{(1)}(\eta, 0)$ for each $k = 1, 2, \cdots, n$ respectively. We assume that the functions are continuous at each interval and use the patching condition

$$f_k^{(l)}(\eta,\zeta_{l-1}) = f_k^{(l-1)}(\eta,\zeta_l) \quad \text{for} \quad k = 1, 2, \cdots, n \quad \text{and} \quad l = 2, 3, \cdots, q \tag{2.2.10}$$

as a new initial condition for the I_l subinterval. The newly adapted system of equations is now given by:

$$\begin{aligned}
&\sum_{s=0}^{p} \alpha_{s,r}^{(1)}(\eta,\zeta) f_{1,r+1}^{(s,l)} + \beta_r^{(1)}(\eta,\zeta)\frac{\partial f_{1,r+1}^{(l)}}{\partial \zeta} + \gamma_r^{(1)}(\eta,\zeta)\frac{\partial f_{1,r+1}^{\prime(l)}}{\partial \zeta} = R_1^{(l)}(\eta,\zeta)\\
&\sum_{s=0}^{p} \alpha_{s,r}^{(2)}(\eta,\zeta) f_{2,r+1}^{(s,l)} + \beta_r^{(2)}(\eta,\zeta)\frac{\partial f_{2,r+1}^{(l)}}{\partial \zeta} + \gamma_r^{(2)}(\eta,\zeta)\frac{\partial f_{2,r+1}^{\prime(l)}}{\partial \zeta} = R_2^{(l)}(\eta,\zeta)\\
&\qquad\qquad\qquad\qquad\vdots\\
&\sum_{s=0}^{p} \alpha_{s,r}^{(n)}(\eta,\zeta) f_{n,r+1}^{(s,l)} + \beta_r^{(n)}(\eta,\zeta)\frac{\partial f_{n,r+1}^{(l)}}{\partial \zeta} + \gamma_r^{(n)}(\eta,\zeta)\frac{\partial f_{2,r+1}^{\prime(l)}}{\partial \zeta} = R_n^{(l)}(\eta,\zeta),
\end{aligned} \tag{2.2.11}$$

where the $l = 1, 2, \cdots, n$ denotes the sub-interval in which the solution belongs.

We assume that the solution can be given in the form:

$$f_k^{(l)}(\eta,\zeta) = \sum_{i=0}^{N_\eta}\sum_{j=0}^{N_\zeta} f(\eta_i,\zeta_j) L_i(\eta) L_j(\zeta) \quad \text{for} \quad k = 1, 2, \cdots, n,$$

where L_i and L_j are Lagrange cardinal polynomials, and η_i and ζ_j are the Chebyshev Gauss-Lobatto grid points. The values of the time derivative at these points are given by:

$$\begin{aligned}
\frac{\partial f_k^{(l)}}{\partial \zeta}(\eta_i,\zeta_j) &= \sum_{p=0}^{N_\eta}\sum_{k=0}^{N_\zeta} f_k^{(l)}(\eta_p,\zeta_k) L_p(\eta_i)\frac{dL_k}{d\zeta}(\zeta_j)\\
&= \sum_{k=0}^{N_\zeta} f_k^{(l)}(\eta_p,\zeta_k) d_{jk}\\
&= \sum_{k=0}^{N_\zeta} d_{jk} f_k^{(l)}(\eta_p,\zeta_k) \quad \text{for} \quad i = 0, 1, .., N_\eta, \quad j = 0, 1, ..., N_\zeta,
\end{aligned}$$

where $d_{jk} = dL_k(\zeta_j)/d\zeta$ is the standard first derivative Chebyshev differentiation matrix of size $(N_\zeta + 1) \times (N_\zeta + 1)$. The values of the space derivatives at the Chebyshev Guass-Lobatto grid points are given by:

$$\begin{aligned}
\frac{\partial f_k^{(l)}}{\partial \eta}(\eta_i,\zeta_j) &= \sum_{p=0}^{N_\eta}\sum_{k=0}^{N_\zeta} f_k^{(l)}(\eta_p,\zeta_k)\frac{dL_p(\eta_i)}{d\eta} L_k(\zeta_j)\\
&= \sum_{k=0}^{N_\zeta} f_k^{(l)}(\eta_p,\zeta_k) D_{ip}\\
&= \sum_{k=0}^{N_\zeta} D_{ip} f_k^{(l)}(\eta_p,\zeta_k) \quad \text{for} \quad i = 0, 1, .., N_\eta, \quad j = 0, 1, ..., N_\zeta
\end{aligned}$$

where $D_{ip} = dL_p(\eta_i)/d\eta$ is the standard first derivative Chebyshev differentiation matrix of size $(N_\eta +$

$1) \times (N_\eta + 1)$. The n^{th} order derivative can be computed as:

$$\frac{\partial^n f_k^{(l)}}{\partial \eta^n}(\eta_i, \zeta_j) = \sum_{k=0}^{N_\zeta} D_{ip}^n f_k^{(l)}(\eta_p, \zeta_k) = \mathbf{D}^n \mathbf{F}_{k,j}^{(l)} \quad \text{for} \quad i = 0, 1, .., N_\eta,$$

where the vector $\mathbf{F}_j^{(l)}$ is defined as $\mathbf{F}_j^{(l)} = [f_j^{(l)}(\eta_0, \zeta_j), f_k^{(l)}(\eta_1, \zeta_j), ..., f_k^{(l)}(\eta_{N_\eta}, \zeta_j)]^T$ for $j = 0, 1, ..., N_\zeta$ and $\mathbf{D}^n$ is the n^{th} derivative Chebyshev differentiation matrix. The superscript T denotes the transpose. Substituting $f_k^{(l)}$ and its derivatives into the first equation of (2.2.11) we obtain:

$$\sum_{s=0}^{3} \boldsymbol{\alpha}_{s,r}^{(1,l)} \mathbf{D}^{(s)} \mathbf{F}_{1,j}^{(l)} + \boldsymbol{\beta}_r^{(1,l)} \sum_{\nu=0}^{N_\zeta} d_{j,\nu} \mathbf{F}_{1,\nu}^{(l)} + \boldsymbol{\gamma}_r^{(1,l)} \sum_{\nu=0}^{N_\zeta} d_{j,\nu} \mathbf{DF}_{1,\nu}^{(l)} = \mathbf{R}_{1,j}^{(l)} \quad \text{for} \quad j = 0, 1, 2, \cdots, N_\zeta \tag{2.2.12}$$

Expanding (2.2.12) for each $j = 0, 1, \cdots, N_\zeta$ we have:

$$\sum_{s=0}^{3} \boldsymbol{\alpha}_{s,r}^{(1,l)} \mathbf{D}^{(s)} \mathbf{F}_{1,0}^{(l)} + \boldsymbol{\beta}_r^{(1,l)} \left(d_{0,0} \mathbf{F}_{1,0}^{(l)} + \cdots + d_{0,N_\zeta} \mathbf{F}_{1,N_\zeta}^{(l)} \right) + \boldsymbol{\gamma}_r^{1,l} \left(d_{0,0} \mathbf{DF}_{1,0}^{(l)} + \cdots + d_{0,N_\zeta} \mathbf{DF}_{1,N_\zeta}^{(l)} \right) = \mathbf{R}_{1,0}^{(l)}$$

$$\sum_{s=0}^{3} \boldsymbol{\alpha}_{s,r}^{(1,l)} \mathbf{D}^{(s)} \mathbf{F}_{1,1}^{(l)} + \boldsymbol{\beta}_r^{(1,l)} \left(d_{1,0} \mathbf{F}_{1,1}^{(l)} + \cdots + d_{1,N_\zeta} \mathbf{F}_{1,N_\zeta}^{(l)} \right) + \boldsymbol{\gamma}_r^{1,l} \left(d_{1,0} \mathbf{DF}_{1,1}^{(l)} + \cdots + d_{1,N_\zeta} \mathbf{DF}_{1,N_\zeta}^{(l)} \right) = \mathbf{R}_{1,1}^{(l)}$$

$$\vdots$$

$$\sum_{s=0}^{3} \boldsymbol{\alpha}_{s,r}^{(1,l)} \mathbf{D}^{(s)} \mathbf{F}_{1,N_\zeta}^{(l)} + \boldsymbol{\beta}_r^{(1,l)} \left(d_{N_\zeta,0} \mathbf{F}_{1,0}^{(l)} + \cdots + d_{N_\zeta,N_\zeta} \mathbf{F}_{1,N_\zeta}^{(l)} \right) + \boldsymbol{\gamma}_r^{1,l} \left(d_{N_\zeta,0} \mathbf{DF}_{1,N_\zeta}^{(l)} + \cdots + d_{N_\zeta,N_\zeta} \mathbf{DF}_{1,N_\zeta}^{(l)} \right) = \mathbf{R}_{1,N_\zeta}^{(l)},$$

which can be written in the form:

$$\mathbf{A}_{1,1}^{(l)} \mathbf{F}_{1,j}^{(l)} + \boldsymbol{\beta}_r^{(1,l)} \sum_{\nu=0}^{N_\zeta} d_{i,j} \mathbf{F}_{1,\nu}^{(l)} + \boldsymbol{\gamma}_r^{(1,l)} \sum_{\nu=0}^{N_\zeta} \mathbf{DF}_{1,\nu}^{(l)} = \mathbf{R}_{1,j}^{(l)} \tag{2.2.13}$$

where:

$$A_{1,1} = \sum_{s=0}^{p} \boldsymbol{\alpha}_{s,r}^{(1,l)} \mathbf{D}^{(s)} \tag{2.2.14}$$

Carrying out the same computation for second up to the n^{th} equation in (2.2.11) we obtain a general system of the form:

$$\begin{aligned}
\mathbf{A}_{1,1}^{(l)} \mathbf{F}_{1,j}^{(l)} + \boldsymbol{\beta}_r^{(1,l)} \sum_{\nu=0}^{N_\zeta} d_{i,j} \mathbf{F}_{1,\nu}^{(l)} + \boldsymbol{\gamma}_r^{(1,l)} \sum_{\nu=0}^{N_\zeta} \mathbf{DF}_{1,\nu}^{(l)} &= \mathbf{R}_{1,j}^{(l)} \\
\mathbf{A}_{2,2}^{(l)} \mathbf{F}_{2,j}^{(l)} + \boldsymbol{\beta}_r^{(2,l)} \sum_{\nu=0}^{N_\zeta} d_{i,j} \mathbf{F}_{2,\nu}^{(l)} + \boldsymbol{\gamma}_r^{(2,l)} \sum_{\nu=0}^{N_\zeta} \mathbf{DF}_{2,\nu}^{(l)} &= \mathbf{R}_{2,j}^{(l)} \\
&\vdots \\
\mathbf{A}_{n,n}^{(l)} \mathbf{F}_{n,j}^{(l)} + \boldsymbol{\beta}_r^{(n,l)} \sum_{\nu=0}^{N_\zeta} d_{i,j} \mathbf{F}_{n,\nu}^{(l)} + \boldsymbol{\gamma}_r^{(n,l)} \sum_{\nu=0}^{N_\zeta} \mathbf{DF}_{n,\nu}^{(l)} &= \mathbf{R}_{n,j}^{(l)},
\end{aligned} \tag{2.2.15}$$

where:

$$A_{1,1} = \sum_{s=0}^{p} \boldsymbol{\alpha}_{s,r}^{(1,l)} \mathbf{D}^{(s)}, \quad A_{2,2} = \sum_{s=0}^{p} \boldsymbol{\alpha}_{s,r}^{(2,l)} \mathbf{D}^{(s)}, \cdots, \quad A_{n,n} = \sum_{s=0}^{p} \boldsymbol{\alpha}_{s,r}^{(n,l)} \mathbf{D}^{(s)}, \tag{2.2.16}$$

the vector $\mathbf{R}_{k,j}^{(l)}$ for $k = 1, 2, \cdots, n$ is given by:

$$\mathbf{R}_{k,j}^{(l)} = [R_k(\eta_0, \zeta_j), R_k(\eta_1, \zeta_j), \cdots, R_k(\eta_{N_\eta}, \zeta_j)]^T. \tag{2.2.17}$$

The diagonal matrices of the corresponding variable coefficients at each k^{th} equation are given by:

$$\boldsymbol{\alpha}_{s,r}^{(1,l)} = \begin{bmatrix} \alpha_{s,r}^{(1,l)}(\eta_0, \zeta_j) & & & \\ & \alpha_{s,r}^{(1,l)}(\eta_1, \zeta_j) & & \\ & & \ddots & \\ & & & \alpha_{s,r}^{(1,l)}(\eta_{N_\eta}, \zeta_j) \end{bmatrix}, \tag{2.2.18}$$

$$\boldsymbol{\beta}_{s,r}^{(1,l)} = \begin{bmatrix} \beta_{s,r}^{(1,l)}(\eta_0, \zeta_j) & & & \\ & \beta_{s,r}^{(1,l)}(\eta_1, \zeta_j) & & \\ & & \ddots & \\ & & & \beta_{s,r}^{(1,l)}(\eta_{N_\eta}, \zeta_j) \end{bmatrix}, \tag{2.2.19}$$

$$\boldsymbol{\gamma}_{s,r}^{(1,l)} = \begin{bmatrix} \gamma_{s,r}^{(1,l)}(\eta_0, \zeta_j) & & & \\ & \gamma_{s,r}^{(1,l)}(\eta_1, \zeta_j) & & \\ & & \ddots & \\ & & & \gamma_{s,r}^{(1,l)}(\eta_{N_\eta}, \zeta_j) \end{bmatrix}. \tag{2.2.20}$$

Recall the patching conditions given by (2.2.10). After collecting like terms and imposing the boundary conditions at each sub-interval we can rewrite the above system in an $N_\zeta(N_\eta+1) \times N_\zeta(N_\eta+1)$ matrix of the form:

$$\begin{bmatrix} B_{0,0}^{(1,l)} & B_{0,1}^{(1,l)} & \cdots & B_{0,N_\zeta-1}^{(1,l)} \\ B_{1,0}^{(1,l)} & B_{1,1}^{(1,l)} & \cdots & B_{1,N_\zeta-1}^{(1,l)} \\ \vdots & \vdots & \ddots & \vdots \\ B_{N_\zeta-1,0}^{(1,l)} & B_{N_\zeta-1,1}^{(1,l)} & \cdots & B_{N_\zeta-1,N_\zeta-1}^{(1,l)} \end{bmatrix} \begin{bmatrix} \boldsymbol{F}_{1,0}^{(l)} \\ \boldsymbol{F}_{1,1}^{(l)} \\ \vdots \\ \boldsymbol{F}_{1,N_\zeta-1}^{(l)} \end{bmatrix} = \begin{bmatrix} \boldsymbol{\mathcal{R}}_{1,0}^{(l)} \\ \boldsymbol{\mathcal{R}}_{1,1}^{(l)} \\ \vdots \\ \boldsymbol{\mathcal{R}}_{1,N_\zeta-1}^{(l)} \end{bmatrix}, \tag{2.2.21}$$

where:

$$\begin{aligned} B_{i,i}^{(1,l)} &= \sum_{s=0}^{3} \boldsymbol{\alpha}_{s,r}^{(1,l)} \mathbf{D}^{(s)} + \boldsymbol{\beta}_r^{(1,l)} d_{i,i} \mathbf{I} + \boldsymbol{\gamma}_r^{(1,l)} d_{i,i} \mathbf{D} \quad \text{for} \quad l = 1, 2, .., p \quad \text{when} \quad i = j, \\ B_{i,j}^{(1,l)} &= \boldsymbol{\beta}_r^{(2,l)} d_{i,j} \mathbf{I} + \boldsymbol{\gamma}_r^{(1,l)} d_{i,j} \mathbf{D} \quad \text{for} \quad l = 1, 2, .., p \quad \text{when} \quad i \neq j, \\ \boldsymbol{\mathcal{R}}_{1,i}^{(l)} &= \mathbf{R}_{1,i}^{(l)} - \left(\boldsymbol{\beta}_r^{(l)} d_{i,N_\zeta} \mathbf{I} + \boldsymbol{\gamma}_r^{(1,l)} d_{i,N_\zeta} \mathbf{D} \right) \mathbf{F}_{1,N_\zeta}^{(l)} \quad \text{for} \quad i = 0, 1, 2, ..., N_\zeta. \end{aligned}$$

A similar computation is carried out for for the second, third up to the n^{th} equation in (2.2.11) and the resultant matrix representation will be given by:

$$\begin{bmatrix} B_{0,0}^{(k,l)} & B_{0,1}^{(k,l)} & \cdots & B_{0,N_\zeta-1}^{(k,l)} \\ B_{1,0}^{(k,l)} & B_{1,1}^{(k,l)} & \cdots & B_{1,N_\zeta-1}^{(k,l)} \\ \vdots & \vdots & \ddots & \vdots \\ B_{N_\zeta-1,0}^{(k,l)} & B_{N_\zeta-1,1}^{(k,l)} & \cdots & B_{N_\zeta-1,N_\zeta-1}^{(k,l)} \end{bmatrix} \begin{bmatrix} \boldsymbol{F}_{k,0}^{(l)} \\ \boldsymbol{F}_{k,1}^{(l)} \\ \vdots \\ \boldsymbol{F}_{k,N_\zeta-1}^{(l)} \end{bmatrix} = \begin{bmatrix} \boldsymbol{\mathcal{R}}_{k,0}^{(l)} \\ \boldsymbol{\mathcal{R}}_{k,1}^{(l)} \\ \vdots \\ \boldsymbol{\mathcal{R}}_{k,N_\zeta-1}^{(l)} \end{bmatrix}, \quad \text{for} \quad k = 2, 3, \cdots, n$$

where:

$$
\begin{aligned}
B_{i,i}^{(k,l)} &= \sum_{s=0}^{3} \boldsymbol{\alpha}_{s,r}^{(k,l)} \mathbf{D}^{(s)} + \boldsymbol{\beta}_{r}^{(k,l)} d_{i,i} \mathbf{I} + \boldsymbol{\gamma}_{r}^{(k,l)} d_{i,i} \mathbf{D} \quad \text{for} \quad l = 1, 2, .., p \quad \text{when} \quad i = j, \\
B_{i,j}^{(k,l)} &= \boldsymbol{\beta}_{r}^{(2,l)} d_{i,j} \mathbf{I} + \boldsymbol{\gamma}_{r}^{(k,l)} d_{i,j} \mathbf{D} \quad \text{for} \quad l = 1, 2, .., p \quad \text{when} \quad i \neq j, \\
\boldsymbol{\mathcal{R}}_{k,i}^{(l)} &= \mathbf{R}_{k,i}^{(l)} - \left(\boldsymbol{\beta}_{r}^{(l)} d_{i,N_\zeta} \mathbf{I} + \boldsymbol{\gamma}_{r}^{(1,l)} d_{i,N_\zeta} \mathbf{D} \right) \mathbf{F}_{k,N_\zeta}^{(l)} \quad \text{for} \quad i = 0, 1, 2, ..., N_\zeta.
\end{aligned}
$$

In the next chapter, we apply the MD-BSLLM to a system of equations modeling the steady free convective flow of a fluid past a non-isothermal vertical porous cone and also to another system of equations modeling the steady free convection flow of a viscous incompressible fluid along a permeable vertical flat surface.

3. Problem Solution Methodology

In this chapter, we test the applicability of the multi-domain bivariate spectral local linearization method as described in chapter 2 by conducting numerical experiments to solve two different flow model equations. The first numerical experiment involves solving the steady free convection flow of a fluid past a non-isothermal vertical porous cone and the second numerical experiment involves solving the steady free convection flow of a viscous incompressible fluid along a permeable vertical flat surface.

This chapter consist of two sections, section 3.1 and section 3.2. In each section, we explain to the reader the mathematical derivation of each of the flow model equations and also apply the MD-BSLLM solution procedure in solving each of the flow model equations.

3.1 Numerical Experiment 1

In this section, we solve the steady free convective flow of a fluid past a non-isothermal vertical porous cone using the MD-BSLLM.

3.1.1 Mathematical Derivations. We consider a two-dimensional free convective flow past a non-isothermal porous cone with variable surface temperature. The effect of viscous dissipation on thermal boundary layer is neglected. The physical co-ordinates (x, y) system for the flow is presented in the figure below:

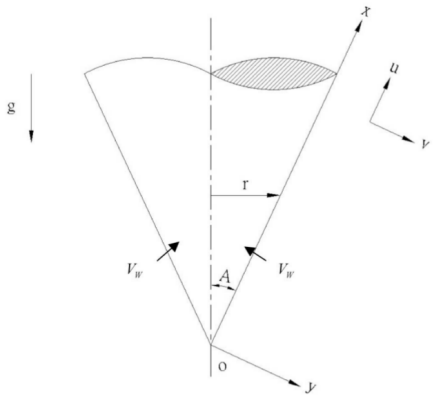

Figure 3.1: Coordinate system [8]

By the Boussinesq approximation of fluid flow [19], the boundary layer approximations governing the fluid flow along the cone are given by:

$$\begin{aligned} \frac{\partial(ru)}{\partial x} + \frac{\partial(rv)}{\partial y} &= 0 \\ u\frac{\partial u}{\partial x} + v\frac{\partial u}{\partial y} &= \nu\frac{\partial^2 u}{\partial y^2} \\ u\frac{\partial T}{\partial x} + u\frac{\partial T}{\partial y} &= \alpha\frac{\partial^2 T}{\partial y^2} \quad , \end{aligned} \tag{3.1.1}$$

where u and v are the fluid velocity components in the x and y directions respectively, ν is the kinematic coefficient of viscosity, g is the acceleration due to gravity, β is the coefficient of volume due to expansion, α is the thermal diffusivity, γ is the cone apex half-angle T is the temperature of the fluid. The boundary conditions are given by:

$$u(x,0)=0, \quad v(x,0)=-V, \quad T(x,0)=T_w(x), \quad u(x,\infty)=0 \quad \text{and} \quad T(x,\infty)=T_\infty. \tag{3.1.2}$$

V_w represents the transpirational velocity of the fluid through the surface of the permeable cone. After writing the governing equations in dimensionless form, we let the Lagrange's stream function Ψ be such that $ru=\dfrac{\partial\Psi}{\partial y}$ and $rv=-\dfrac{\partial\Psi}{\partial x}$ and also satisfy (3.1.1). We then reduce the dimensionless governing partial differential equations to ordinary differential equations by finding a change of variables which allows us to perform the reduction. We look for a one-parameter transformation of variables y, x and Ψ under which the equations for the resultant boundary value problem after substituting Ψ are invariant. We define the transformation variables as follows:

$$\zeta=\nu\frac{V_w x}{Gr^{1/4}}, \quad \eta=Gr^{1/4}\left(\frac{y}{x}\right), \quad \Psi=\nu r(Gr^{1/4})\left(f+\frac{\zeta}{2}\right), \quad \theta=\frac{T-T_\infty}{T_w-T_\infty}, \tag{3.1.3}$$

as defined by Cheng [8], where ζ represents the suction variable and $Gr=\dfrac{s\beta(T_w-T_\infty)}{\nu^2}$ is the Grashof number [34]. For a small boundary thickness relative to the radius of the cone, the local radius to a point in the boundary layer can be approximated by:

$$r=x\sin A. \tag{3.1.4}$$

Substituting (3.1.3) and (3.1.4) into the governing equations we obtain

$$\begin{aligned}
&\frac{1}{1+E\theta}f'''-\frac{E}{(1+E\theta)^2}f''\theta'+\frac{n+7}{4}ff''-\frac{n+1}{2}(f')^2+\theta+\zeta f''=\frac{1-n}{4}\zeta\left(f'\frac{\partial f'}{\partial\zeta}-f''\frac{\partial f}{\partial\zeta}\right),\\
&\frac{1}{Pr}\theta'' \quad + \quad \frac{n+7}{4}f\theta'-nf'\theta+\zeta\theta'=\frac{1-n}{4}\zeta\left(f'\frac{\partial\theta}{\partial\zeta}-\theta'\frac{\partial f}{\partial\zeta}\right),
\end{aligned}$$

where the primes denotes the the partial derivation with respect to η, $\quad Pr=\nu/\alpha$ is the Prandtl number [19] and E is the energy. For a free convectional flow of a fluid past a non-isothermal vertical porous cone with variable surface temperature, $E=0$ and hence the governing equations become:

$$\begin{aligned}
&f'''+\frac{n+7}{4}ff''-\frac{n+1}{2}(f')^2+\theta+\zeta f''=\frac{1-n}{4}\zeta\left(f'\frac{\partial f'}{\partial\zeta}-f''\frac{\partial f}{\partial\zeta}\right),\\
&\frac{1}{Pr}\theta''+\frac{n+7}{4}f\theta'-nf'\theta+\zeta\theta'=\frac{1-n}{4}\zeta\left(f'\frac{\partial\theta}{\partial\zeta}-\theta'\frac{\partial f}{\partial\zeta}\right),
\end{aligned} \tag{3.1.5}$$

as presented in [17]. The corresponding boundary conditions are given by:

$$f(\zeta,0)=0, \quad f'(\zeta,0)=0, \quad \theta(\zeta,0)=1, \quad f'(\zeta,\infty)=0, \quad \theta(\zeta,\infty)=0. \tag{3.1.6}$$

The skin friction C_{fx} and the Nusselt number Nu_x are the most important parameters to be determined. The skin friction describes the shear stress while the Nusselt number tells us about the heat flux rate at the surface of the medium. These parameters have been defined in [17] as follows:

$$C_{fx}Gr_x^{1/4}=f''(\zeta,0), \quad \frac{Nu_x}{Gr_x^{1/4}}=-\theta'(\zeta,0). \tag{3.1.7}$$

3.1.2 Solution Procedure. To apply the spectral local linearization method to equation (3.1.5), we let $f(\eta,\zeta)=f_1(\eta,\zeta)$ and $\theta(\eta,\zeta)=f_2(\eta,\zeta)$ and rewrite (3.1.5) in the form:

$$\Gamma_1 = f_1^{(3,l)} + \frac{n+7}{4} f_1^{(0,l)} f_1^{(2,l)} - \frac{n+1}{2}(f_1^{(1,l)})^2 + f_2^{(0,l)} + \zeta f_1^{(2,l)} - \frac{1-n}{4}\zeta\left(f_1^{(1,l)}\frac{\partial f_1^{(1,l)}}{\partial\zeta} - f_1^{(2,l)}\frac{\partial f_1^{(0,l)}}{\partial\zeta}\right),$$
$$\Gamma_2 = \frac{1}{Pr} f_2^{(2,l)} + \frac{n+7}{4} f_1 f_2^{(1,l)} - n f_1^{(1,l)} f_2^{(0,l)} + \zeta f_2^{(1,l)} - \frac{1-n}{4}\zeta\left(f_1^{(0,l)}\frac{\partial f_2^{(0,l)}}{\partial\zeta} - f_2^{(1,l)}\frac{\partial f_1^{(0,l)}}{\partial\zeta}\right). \tag{3.1.8}$$

The order of differentiation $p=3$ and the number of equations in the system $n=2$. We compute the variable coefficients $\alpha_{s,r}^{(k,l)}(\eta,\zeta)$, $\beta_r^{(k,l)}(\eta,\zeta)$ and $\gamma_r^{(k,l)}(\eta,\zeta)$ for $k=1,2$ and $s=0,1,2,3$. For $k=1$, we have:

$$\alpha_{0,r}^{(1,l)}(\eta,\zeta) = \frac{\partial\Gamma_1}{\partial f_{1,r}^{(0,l)}} = \frac{n+7}{4} f_{1,r}^{(2,l)}, \quad \alpha_{1,r}^{(1,l)}(\eta,\zeta) = \frac{\partial\Gamma_1}{\partial f_{1,r}^{(1,l)}} = -(n+1) f_{1,r}^{(1,l)} - \frac{1-n}{4}\zeta\frac{\partial f_{1,r}^{(1,l)}}{\partial\zeta},$$
$$\alpha_{2,r}^{(1,l)}(\eta,\zeta) = \frac{\partial\Gamma_1}{\partial f_{1,r}^{(2,l)}} = \frac{n+7}{4} f_{1,r}^{(0,l)} + \zeta + \frac{1-n}{4}\zeta\frac{\partial f_{1,r}^{(1,l)}}{\partial\zeta}, \quad \alpha_{3,r}^{(1,l)}(\eta,\zeta) = \frac{\partial\Gamma_1}{\partial f_{1,r}^{(3,l)}} = 1,$$
$$\beta_r^{(1)}(\eta,\zeta) = \frac{\partial\Gamma_1}{\partial\left(\dfrac{\partial f_{1,r}^{(0,l)}}{\partial\zeta}\right)} = \frac{1-n}{4}\zeta f_{1,r}^{(2,l)}, \quad \gamma_r^{(1,l)} = \frac{\partial\Gamma_1}{\partial\left(\dfrac{\partial f_{1,r}^{(1,l)}}{\partial\zeta}\right)} = -\frac{1-n}{4}\zeta f_{1,r}^{(1,l)} \tag{3.1.9}$$

for $k=2$,

$$\alpha_{0,r}^{(2)}(\eta,\zeta) = \frac{\partial\Gamma_2}{\partial f_{2,r}^{(0,l)}} = -n f_{1,r}^{(1,l)}, \quad \alpha_{1,r}^{(2,l)}(\eta,\zeta) = \frac{\partial\Gamma_2}{\partial f_{2,r}^{(1,l)}} = \frac{n+7}{4} f_{1,r}^{(0,l)} + \zeta + \frac{1-n}{4}\zeta\frac{\partial f_{1,r}^{(0,l)}}{\partial\zeta},$$
$$\alpha_{2,r}^{(2,l)}(\eta,\zeta) = \frac{\partial\Gamma_2}{\partial f_{2,r}^{(2,l)}} = \frac{1}{Pr}, \quad \alpha_{3,r}^{(2,l)}(\eta,\zeta) = \frac{\partial\Gamma_2}{\partial f_{2,r}^{(3,l)}} = 0, \quad \gamma_r^{(2,l)}(\eta,\zeta) = \frac{\partial\Gamma_2}{\partial\left(\dfrac{\partial f_{2,r}^{(1,l)}}{\partial\zeta}\right)} = 0$$
$$\beta_r^{(2,l)}(\eta,\zeta) = \frac{\partial\Gamma_2}{\partial\left(\dfrac{\partial f_{2,r}^{(0,l)}}{\partial\zeta}\right)} = -\frac{1-n}{4}\zeta f_{2,r}^{(0,l)}. \tag{3.1.10}$$

The linearized form of (3.1.8) is then written in the form:

$$\sum_{s=0}^{3}\alpha_{s,r}^{(1,l)}(\eta,\zeta) f_{1,r+1}^{(s,l)} + \beta_r^{(1,l)}(\eta,\zeta)\frac{\partial f_{1,r+1}^{(0,l)}}{\partial\zeta} + \gamma_r^{(1,l)}(\eta,\zeta)\frac{\partial f_{1,r+1}^{(1,l)}}{\partial\zeta} = R_1^{(l)}(\eta,\zeta) \tag{3.1.11}$$
$$\sum_{s=0}^{3}\alpha_{s,r}^{(2,l)}(\eta,\zeta) f_{2,r+1}^{(s,l)} + \beta_r^{(2,l)}(\eta,\zeta)\frac{\partial f_{2,r+1}^{(0,l)}}{\partial\zeta} + \gamma_r^{(2,l)}(\eta,\zeta)\frac{\partial f_{2,r+1}^{(1,l)}}{\partial\zeta} = R_2^{(l)}(\eta,\zeta) \tag{3.1.12}$$

Taking into account the patching and boundary conditions as illustrated in the previous section, the matrix system of equations for (3.1.11) and (3.1.12) to be solved are:

$$\begin{bmatrix} B_{0,0}^{(1,l)} & B_{0,1}^{(1,l)} & \cdots & B_{0,N_\zeta-1}^{(1,l)} \\ B_{1,0}^{(1,l)} & B_{1,1}^{(1,l)} & \cdots & B_{1,N_\zeta-1}^{(1,l)} \\ \vdots & \vdots & \ddots & \vdots \\ B_{N_\zeta-1,0}^{(1,l)} & B_{N_\zeta-1,1}^{(1,l)} & \cdots & B_{N_\zeta-1,N_\zeta-1}^{(1,l)} \end{bmatrix} \begin{bmatrix} \boldsymbol{F}_{1,0}^{(l)} \\ \boldsymbol{F}_{1,1}^{(l)} \\ \vdots \\ \boldsymbol{F}_{1,N_\zeta-1}^{(l)} \end{bmatrix} = \begin{bmatrix} \boldsymbol{\mathcal{R}}_{1,0}^{(l)} \\ \boldsymbol{\mathcal{R}}_{1,1}^{(l)} \\ \vdots \\ \boldsymbol{\mathcal{R}}_{1,N_\zeta-1}^{(l)} \end{bmatrix},$$
$$\begin{bmatrix} B_{0,0}^{(2,l)} & B_{0,1}^{(2,l)} & \cdots & B_{0,N_\zeta-1}^{(2,l)} \\ B_{1,0}^{(2,l)} & B_{1,1}^{(2,l)} & \cdots & B_{1,N_\zeta-1}^{(2,l)} \\ \vdots & \vdots & \ddots & \vdots \\ B_{N_\zeta-1,0}^{(2,l)} & B_{N_\zeta-1,1}^{(2,l)} & \cdots & B_{N_\zeta-1,N_\zeta-1}^{(2,l)} \end{bmatrix} \begin{bmatrix} \boldsymbol{F}_{2,0}^{(l)} \\ \boldsymbol{F}_{2,1}^{(l)} \\ \vdots \\ \boldsymbol{F}_{2,N_\zeta-1}^{(l)} \end{bmatrix} = \begin{bmatrix} \boldsymbol{\mathcal{R}}_{2,0}^{(l)} \\ \boldsymbol{\mathcal{R}}_{2,1}^{(l)} \\ \vdots \\ \boldsymbol{\mathcal{R}}_{2,N_\zeta-1}^{(l)} \end{bmatrix}, \tag{3.1.13}$$

respectively, where:

$$\begin{aligned}
B_{i,i}^{(1,l)} &= \sum_{s=0}^{3} \boldsymbol{\alpha}_{s,r}^{(1,l)} \mathbf{D}^{(s)} + \boldsymbol{\beta}_r^{(1,l)} d_{i,i} \mathbf{I} + \boldsymbol{\gamma}_r^{(1,l)} d_{i,i} \mathbf{D} \quad \text{for} \quad l = 1, 2, .., p \quad \text{when} \quad i = j, \\
B_{i,j}^{(1,l)} &= \boldsymbol{\beta}_r^{(2,l)} d_{i,j} \mathbf{I} + \boldsymbol{\gamma}_r^{(,l)} d_{i,j} \mathbf{D} \quad \text{for} \quad l = 1, 2, .., p \quad \text{when} \quad i \neq j, \\
\boldsymbol{\mathcal{R}}_{1,i}^{(l)} &= \mathbf{R}_{1,i}^{(l)} - \left(\boldsymbol{\beta}_r^{(l)} d_{i,N_\zeta} \mathbf{I} + \boldsymbol{\gamma}_r^{(1,l)} d_{i,N_\zeta} \mathbf{D} \right) \mathbf{F}_{1,N_\zeta}^{(l)} \quad \text{for} \quad = 0, 1, 2, ..., N_\zeta, \\
B_{i,i}^{(2,l)} &= \sum_{s=0}^{3} \boldsymbol{\alpha}_{s,r}^{(2,l)} \mathbf{D}^{(s)} + \boldsymbol{\beta}_r^{(2,l)} d_{i,i} \mathbf{I} + \boldsymbol{\gamma}_r^{(2,l)} d_{i,i} \mathbf{D} \quad \text{for} \quad l = 1, 2, .., p \quad \text{when} \quad i = j, \\
B_{i,j}^{(2,l)} &= \boldsymbol{\beta}_r^{(2,l)} d_{i,j} \mathbf{I} + \boldsymbol{\gamma}_r^{(2,l)} d_{i,j} \mathbf{D} \quad \text{for} \quad l = 1, 2, .., p \quad \text{when} \quad i \neq j, \\
\boldsymbol{\mathcal{R}}_{2,i}^{(l)} &= \mathbf{R}_{2,i}^{(l)} - \left(\boldsymbol{\beta}_r^{(l)} d_{i,N_\zeta} \mathbf{I} + \boldsymbol{\gamma}_r^{(1,l)} d_{i,N_\zeta} \mathbf{D} \right) \mathbf{F}_{2,N_\zeta}^{(l)} \quad \text{for} \quad i = 0, 1, 2, ..., N_\zeta,
\end{aligned}$$

$\mathbf{I}$ is an $N_\eta(N_\zeta + 1) \times N_\eta(N_\zeta + 1)$ identity matrix.

3.2 Numerical Experiment 2

In this section, we solve the steady convective flow of a viscous incompressible fluid along a permeable vertical flat surface using the MD-BSLLM.

3.2.1 Mathematical Derivations. In this case, we consider a two-dimensional steady free convective flow of a viscous incompressible fluid along a permeable vertical flat plate in the presence of a soluble species. The coordinate system and the configuration is shown below in Figure 3.2. By the Boussinesq approximation of fluid flow [19], the heat and mass transfer processes of the system are governed by

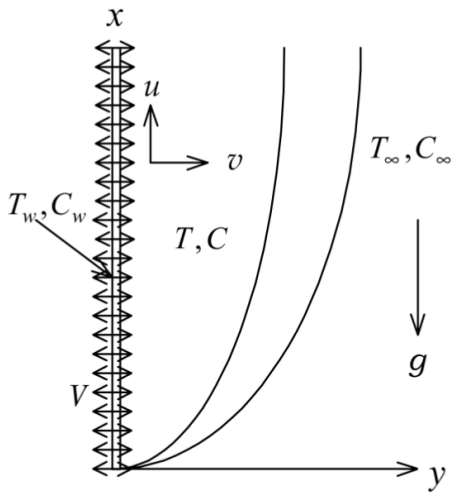

Figure 3.2: Physical configuration and coordinate system [19]

the following set of equations:

$$\frac{\partial u}{\partial x} + \frac{\partial v}{\partial y} = 0 \tag{3.2.1}$$

$$u\frac{\partial u}{\partial x} + v\frac{\partial u}{\partial y} = \nu\frac{\partial^2 u}{\partial y^2} + g(\beta_T\theta + \beta_C\phi) \tag{3.2.2}$$

$$u\frac{\partial \theta}{\partial x} + v\frac{\partial \theta}{\partial y} = \alpha\frac{\partial^2 \theta}{\partial y^2} \tag{3.2.3}$$

$$u\frac{\partial \phi}{\partial x} + v\frac{\partial \phi}{\partial y} = D\frac{\partial^2 \phi}{\partial y^2} \tag{3.2.4}$$

and the boundary conditions are given by:

$$\begin{aligned} &u(x,0) = 0, \quad v(x,0) = -V, \quad \theta(x,0) = \theta_0 x^n, \quad \phi(x,0) = \phi_0 x^n, \\ &u(x,y) = 0, \quad \theta = 0, \quad \phi = 0 \quad \text{at} \quad y = \infty, \end{aligned} \tag{3.2.5}$$

where u and v represent the x and y components of the velocity field respectively, β_T and β_C are the volumetric expansion coefficients for temperature and concentration respectively, g is the gravitational acceleration, α is the thermal diffusivity and D is the molecular diffusivity of the species concentration, $V \geq 0$ is the suction velocity of the fluid through the surface of plate. θ_0 and ϕ_0 are respectively the constant temperature and constant species concentration at the surface of the plate. After writing the governing equations in dimensionless form, we let the Lagrange's stream function Ψ be such that $u = \dfrac{\partial \Psi}{\partial y}$ and $v = -\dfrac{\partial \Psi}{\partial x}$ and also satisfy (3.2.1). We then reduce the dimensionless governing partial differential equations to ordinary differential equations by finding a change of variables which allows us to perform the reduction. We look for a one-parameter transformation of variables y, x and Ψ under which the equations for the resultant boundary value problem after substituting Ψ are invariant. We define the transformation variables as follows (see Hussain [19]):

$$\begin{aligned} &\eta = Gr_x^{1/4}\left(\frac{y}{x}\right), \quad \zeta = Gr_x^{1/4}\left(\frac{V_x}{\nu}\right), \quad \phi(x,y) = h(\zeta,\eta), \\ &\theta(x,y) = g(\zeta,\eta), \quad \Psi(x,y) = \nu Gr_x^{1/4}(f(\zeta,\eta) + \zeta). \end{aligned} \tag{3.2.6}$$

The functions f, g, h are the non-dimensional stream functions, temperature and concentration functions respectively, η is the pseudo-similarity variable and ζ is the transpirational parameter. We define

$$Gr_x = \frac{g(\beta_T\theta_w + \beta_C\phi_w)}{\nu^2}x^3 = Gr_{x,T} + Gr_{x,C} \tag{3.2.7}$$

as the modified Grashof number, with $Gr_{x,T}$ and $Gr_{x,C}$ being the local Grashof number for thermal diffusion and Grashof number for mass diffusion respectively. After substituting the transformations (3.2.6) into (3.2.1) - (3.2.4), we obtain the following non-similarity equations:

$$\begin{aligned}
&f''' + \frac{n+3}{4}ff'' - \frac{n+1}{2}f'^2 + (1-w)g + wh = \frac{1-n}{4}\zeta\left(f'\frac{\partial f'}{\partial\zeta} - f''\frac{\partial f}{\partial\zeta}\right),\\
&\frac{1}{Pr}g'' + \frac{n+3}{4}fg' + \zeta g' = \frac{1-n}{4}\zeta\left(f'\frac{\partial g}{\partial\zeta} - g'\frac{\partial f}{\partial\zeta}\right),\\
&\frac{1}{Sc}h'' + \frac{n+3}{4}fh' + \zeta h' = \frac{1-n}{4}\zeta\left(f'\frac{\partial h}{\partial\zeta} - h'\frac{\partial f}{\partial\zeta}\right),
\end{aligned} \tag{3.2.8}$$

where the primes denote the derivation of the functions with respect to η, w measures the relative importance of solutal and thermal diffusion in causing the density changes which drive the flow and is given by:

$$w = \frac{N}{N+1}, \quad \text{where} \quad N = \frac{Gr_{x,C}}{Gr_{x,T}}. \tag{3.2.9}$$

The appropriate boundary conditions are given by:

$$f(\zeta,0) = f'(\zeta,0) = 0, \quad g(\zeta,0) = h(\zeta,0) = 1, \quad f'(\zeta,\infty) = g(\zeta,\infty) = h(\zeta,\infty) = 0. \tag{3.2.10}$$

Pr is the Prandtl number and Sc is the Schmidt number. The physical parameters of interest include the skin friction, Nusselt number and the Sherwood number, which are defined by [17] as:

$$C_{f,x}Gr_x^{3/4} = f''(\zeta,0), \quad Nu_xGr_x^{-1/4} = -g'(\zeta), \quad Sh_xGr^{-1/4} = -h'(\zeta) \tag{3.2.11}$$

respectively.

3.2.2 Solution Procedure. To apply the spectral local linearization method, we let $f(\zeta,\eta) = f_1(\zeta,\eta), \quad g(\zeta,\eta) = f_2(\zeta,\eta)$ and $h(\zeta,\eta) = f_3(\zeta,\eta)$ and rewrite the governing equations in the form:

$$\begin{aligned}
\Gamma_1 &= f_1^{(3,l)} + \frac{n+3}{4}f_1^{(0,l)}f_1^{(2,l)} - \frac{n+1}{2}(f_1^{(1,l)})^2 + (1-w)f_2^{(0,l)} + wf_3^{(0,l)}\\
&\quad - \frac{1-n}{4}\zeta\left(f_1^{(1,l)}\frac{\partial f_1^{(1,l)}}{\partial\zeta} - f_1^{(2,l)}\frac{\partial f_1^{(0,l)}}{\partial\zeta}\right)\\
\Gamma_2 &= \frac{1}{Pr}f_2^{(2,l)} + \frac{n+3}{4}f_1^{(0,l)}f_2^{(1,l)} + \zeta f_2^{(1,l)} - \frac{1-n}{4}\zeta\left(f_1^{(0,l)}\frac{\partial f_2^{(0,l)}}{\partial\zeta} - f_2^{(1,l)}\frac{\partial f_1^{(0,l)}}{\partial\zeta}\right)\\
\Gamma_3 &= \frac{1}{Sc}f_3^{(2,l)} + \frac{n+3}{4}f_1^{(0,l)}f_3^{(1,l)} + \zeta f_3^{(1,l)} - \frac{1-n}{4}\zeta\left(f_1^{(0,l)}\frac{\partial f_2^{(0,l)}}{\partial\zeta} - f_3^{(1,l)}\frac{\partial f_1^{(0,l)}}{\partial\zeta}\right)
\end{aligned} \tag{3.2.12}$$

The order of differentiation in the above system $p = 3$ and the number of equations $n = 3$. The coefficient variables $\alpha_{s,r}^{(k,l)}(\eta,\zeta), \beta_r^{(k,l)}(\eta,\zeta)$ and $\gamma_r^{(k,l)}(\eta,\zeta)$ for $k = 1,2,3$ and $s = 0,1,2,3.$ are given

as: For $k=1$,

$$\begin{aligned}
&\alpha_{0,r}^{(1,l)}=\frac{\partial\Gamma_1}{\partial f_{1,r}^{(0,l)}}=\left(\frac{n+3}{4}\right)f_{1,r}^{(2,l)},\quad \alpha_{1,r}^{(1,l)}=\frac{\partial\Gamma_1}{\partial f_{1,r}^{(1,l)}}=-(n+1)f_{1,r}^{(1,l)}-\frac{1-n}{4}\zeta\frac{\partial f_{1,r}^{(1,l)}}{\partial\zeta}\\
&\alpha_{2,r}^{(1,l)}=\frac{\partial\Gamma_1}{\partial f_{1,r}^{(2,l)}}=\left(\frac{n+3}{4}\right)f_{1,r}^{(0,l)}+\left(\frac{1-n}{4}\right)\zeta\frac{\partial f_{1,r}^{(0,l)}}{\partial\zeta},\quad \alpha_{3,r}^{(1,l)}=\frac{\partial\Gamma_1}{\partial f_{1,r}^{(3,l)}}=1\\
&\beta_{r}^{(1,l)}=\frac{\partial\Gamma_1}{\partial\left(\frac{\partial f_{1,r}^{(0,l)}}{\partial\zeta}\right)}=\left(\frac{1-n}{4}\right)\zeta f_{1,r}^{(2,l)},\quad \gamma_{r}^{(1,l)}=\frac{\partial\Gamma_1}{\partial\left(\frac{\partial f_{1,r}^{(1,l)}}{\partial\zeta}\right)}=-\left(\frac{1-n}{4}\right)\zeta f_{1,r}^{(0,l)},
\end{aligned}\qquad (3.2.13)$$

for $k=2$,

$$\begin{aligned}
&\alpha_{0,r}^{(2,l)}=\frac{\partial\Gamma_2}{\partial f_{2,r}^{(0,l)}}=0,\quad \alpha_{1,r}^{(2,l)}=\frac{\partial\Gamma_2}{\partial f_{2,r}^{(1,l)}}=\left(\frac{n+3}{4}\right)f_{1,r}^{(0,l)}+\zeta+\left(\frac{1-n}{4}\right)\zeta\frac{\partial f_{1,r}^{(0,l)}}{\partial\zeta},\\
&\alpha_{2,r}^{(2,l)}=\frac{\partial\Gamma_2}{\partial f_{2,r}^{(2,l)}}=\frac{1}{Pr},\quad \alpha_{3,r}^{(2,l)}=\frac{\partial\Gamma_2}{\partial f_{2,r}^{(3,l)}}=0,\quad \gamma_{r}^{(2,l)}=\frac{\partial\Gamma_2}{\partial\left(\frac{\partial f_{2,r}^{(1,l)}}{\partial\zeta}\right)}=0,\\
&\beta_{r}^{(2,l)}=\frac{\partial\Gamma_2}{\partial\left(\frac{\partial f_{2,r}^{(0,l)}}{\partial\zeta}\right)}=-\left(\frac{1-n}{4}\right)\zeta f_{1,r}^{(0,l)},
\end{aligned}\qquad (3.2.14)$$

for $k=3$,

$$\begin{aligned}
&\alpha_{0,r}^{(3,l)}=\frac{\partial\Gamma_3}{\partial f_{3,r}^{(0,l)}}=0,\quad \alpha_{1,r}^{(3,l)}=\frac{\partial\Gamma_3}{\partial f_{3,r}^{(1,l)}}=\left(\frac{n+3}{4}\right)f_{1,r}^{(0,l)}+\zeta+\left(\frac{1-n}{4}\right)\zeta\frac{\partial f_{1,r}^{(0,l)}}{\partial\zeta},\\
&\alpha_{2,r}^{(3,l)}=\frac{\partial\Gamma_3}{\partial f_{3,r}^{(2,l)}}=\frac{1}{Sc},\quad \alpha_{3,r}^{(3,l)}=\frac{\partial\Gamma_3}{\partial f_{3,r}^{(3,l)}}=0,\quad \gamma_{r}^{(3,l)}=\frac{\partial\Gamma_3}{\partial\left(\frac{\partial f_{3,r}^{(1,l)}}{\partial\zeta}\right)}=0,\\
&\beta_{r}^{(3,l)}=\frac{\partial\Gamma_3}{\partial\left(\frac{\partial f_{3,r}^{(0,l)}}{\partial\zeta}\right)}=-\left(\frac{1-n}{4}\right)\zeta f_{1,r}^{(0,l)}.
\end{aligned}\qquad (3.2.15)$$

The linearized form of (3.2.12)-(3.2.12) is given by:

$$\sum_{s=0}^{3}\alpha_{s,r}^{(1,l)}(\eta,\zeta)f_{1,r+1}^{(s,l)}+\beta_{r}^{(1,l)}(\eta,\zeta)\frac{\partial f_{1,r+1}^{0,l}}{\partial\zeta}+\gamma_{r}^{(1,l)}(\eta,\zeta)\frac{\partial f_{1,r+1}^{(1,l)}}{\partial\zeta}=R_1^{(l)}(\eta,\zeta)\qquad (3.2.16)$$

$$\sum_{s=0}^{3}\alpha_{s,r}^{(2,l)}(\eta,\zeta)f_{2,r+1}^{(s,l)}+\beta_{r}^{(2,l)}(\eta,\zeta)\frac{\partial f_{2,r+1}^{(0,l)}}{\partial\zeta}+\gamma_{r}^{(2,l)}(\eta,\zeta)\frac{\partial f_{2,r+1}^{(1,l)}}{\partial\zeta}=R_2^{(l)}(\eta,\zeta)\qquad (3.2.17)$$

$$\sum_{s=0}^{3}\alpha_{s,r}^{(3,l)}(\eta,\zeta)f_{3,r+1}^{(s,l)}+\beta_{r}^{(3,l)}(\eta,\zeta)\frac{\partial f_{3,r+1}^{(0,l)}}{\partial\zeta}+\gamma_{r}^{(3,l)}(\eta,\zeta)\frac{\partial f_{3,r+1}^{(1,l)}}{\partial\zeta}=R_3^{(l)}(\eta,\zeta)\qquad (3.2.18)$$

Taking into account the patching and the boundary conditions, the equations (3.2.16), (3.2.17) and (3.2.18) can be expressed in the matrix forms:

$$\begin{bmatrix} B_{0,0}^{(1,l)} & B_{0,1}^{(1,l)} & \cdots & B_{0,N_\zeta-1}^{(1,l)} \\ B_{1,0}^{(1,l)} & B_{1,1}^{(1,l)} & \cdots & B_{1,N_\zeta-1}^{(1,l)} \\ \vdots & \vdots & \ddots & \vdots \\ B_{N_\zeta-1,0}^{(1,l)} & B_{N_\zeta-1,1}^{(1,l)} & \cdots & B_{N_\zeta-1,N_\zeta-1}^{(1,l)} \end{bmatrix} \begin{bmatrix} \boldsymbol{F}_{1,0}^{(l)} \\ \boldsymbol{F}_{1,1}^{(l)} \\ \vdots \\ \boldsymbol{F}_{1,N_\zeta-1}^{(l)} \end{bmatrix} = \begin{bmatrix} \boldsymbol{\mathcal{R}}_{1,0}^{(l)} \\ \boldsymbol{\mathcal{R}}_{1,1}^{(l)} \\ \vdots \\ \boldsymbol{\mathcal{R}}_{1,N_\zeta-1}^{(l)} \end{bmatrix},$$

$$\begin{bmatrix} B_{0,0}^{(2,l)} & B_{0,1}^{(2,l)} & \cdots & B_{0,N_\zeta-1}^{(2,l)} \\ B_{1,0}^{(2,l)} & B_{1,1}^{(2,l)} & \cdots & B_{1,N_\zeta-1}^{(2,l)} \\ \vdots & \vdots & \ddots & \vdots \\ B_{N_\zeta-1,0}^{(2,l)} & B_{N_\zeta-1,1}^{(2,l)} & \cdots & B_{N_\zeta-1,N_\zeta-1}^{(2,l)} \end{bmatrix} \begin{bmatrix} \boldsymbol{F}_{2,0}^{(l)} \\ \boldsymbol{F}_{2,1}^{(l)} \\ \vdots \\ \boldsymbol{F}_{2,N_\zeta-1}^{(l)} \end{bmatrix} = \begin{bmatrix} \boldsymbol{\mathcal{R}}_{2,0}^{(l)} \\ \boldsymbol{\mathcal{R}}_{2,1}^{(l)} \\ \vdots \\ \boldsymbol{\mathcal{R}}_{2,N_\zeta-1}^{(l)} \end{bmatrix}, \tag{3.2.19}$$

$$\begin{bmatrix} B_{0,0}^{(3,l)} & B_{0,1}^{(3,l)} & \cdots & B_{0,N_\zeta-1}^{(3,l)} \\ B_{1,0}^{(3,l)} & B_{1,1}^{(3,l)} & \cdots & B_{1,N_\zeta-1}^{(3,l)} \\ \vdots & \vdots & \ddots & \vdots \\ B_{N_\zeta-1,0}^{(3,l)} & B_{N_\zeta-1,1}^{(3,l)} & \cdots & B_{N_\zeta-1,N_\zeta-1}^{(3,l)} \end{bmatrix} \begin{bmatrix} \boldsymbol{F}_{3,0}^{(l)} \\ \boldsymbol{F}_{3,1}^{(l)} \\ \vdots \\ \boldsymbol{F}_{3,N_\zeta-1}^{(l)} \end{bmatrix} = \begin{bmatrix} \boldsymbol{\mathcal{R}}_{3,0}^{(l)} \\ \boldsymbol{\mathcal{R}}_{3,1}^{(l)} \\ \vdots \\ \boldsymbol{\mathcal{R}}_{3,N_\zeta-1}^{(l)} \end{bmatrix},$$

respectively, where:

$$\begin{aligned}
B_{i,i}^{(1,l)} &= \sum_{s=0}^{3} \boldsymbol{\alpha}_{s,r}^{(1,l)} \mathbf{D}^{(s)} + \boldsymbol{\beta}_r^{(1,l)} d_{i,i} \mathbf{I} + \boldsymbol{\gamma}_r^{(1,l)} d_{i,i} \mathbf{D} \quad \text{for} \quad l = 1, 2, .., p \quad \text{when} \quad i = j, \\
B_{i,j}^{(1,l)} &= \boldsymbol{\beta}_r^{(2,l)} d_{i,j} \mathbf{I} + \boldsymbol{\gamma}_r^{(,l)} d_{i,j} \mathbf{D} \quad \text{for} \quad l = 1, 2, .., p \quad \text{for} \quad i \neq j, \\
\boldsymbol{\mathcal{R}}_{1,i}^{(l)} &= \mathbf{R}_{1,i}^{(l)} - \left(\boldsymbol{\beta}_r^{(l)} d_{i,N_\zeta} \mathbf{I} + \boldsymbol{\gamma}_r^{(1,l)} d_{i,N_\zeta} \mathbf{D} \right) \mathbf{F}_{1,N_\zeta}^{(l)} \quad \text{for} \quad i = 0, 1, 2, ..., N_\zeta, \\
B_{i,i}^{(2,l)} &= \sum_{s=0}^{3} \boldsymbol{\alpha}_{s,r}^{(2,l)} \mathbf{D}^{(s)} + \boldsymbol{\beta}_r^{(2,l)} d_{i,i} \mathbf{I} + \boldsymbol{\gamma}_r^{(2,l)} d_{i,i} \mathbf{D} \quad \text{for} \quad l = 1, 2, .., p \quad \text{when} \quad i = j, \\
B_{i,j}^{(2,l)} &= \boldsymbol{\beta}_r^{(2,l)} d_{i,j} \mathbf{I} + \boldsymbol{\gamma}_r^{(2,l)} d_{i,j} \mathbf{D} \quad \text{for} \quad l = 1, 2, .., p \quad \text{when} \quad i \neq j, \\
\boldsymbol{\mathcal{R}}_{2,i}^{(l)} &= \mathbf{R}_{2,i}^{(l)} - \left(\boldsymbol{\beta}_r^{(l)} d_{i,N_\zeta} \mathbf{I} + \boldsymbol{\gamma}_r^{(2,l)} d_{i,N_\zeta} \mathbf{D} \right) \mathbf{F}_{2,N_\zeta}^{(l)} \quad \text{for} \quad i = 0, 1, 2, ..., N_\zeta. \\
B_{i,i}^{(3,l)} &= \sum_{s=0}^{3} \boldsymbol{\alpha}_{s,r}^{(3,l)} \mathbf{D}^{(s)} + \boldsymbol{\beta}_r^{(3,l)} d_{i,i} \mathbf{I} + \boldsymbol{\gamma}_r^{(3,l)} d_{i,i} \mathbf{D} \quad \text{for} \quad l = 1, 2, .., p \quad \text{when} \quad i = j, \\
B_{i,j}^{(3,l)} &= \boldsymbol{\beta}_r^{(3,l)} d_{i,j} \mathbf{I} + \boldsymbol{\gamma}_r^{(3,l)} d_{i,j} \mathbf{D} \quad \text{for} \quad l = 1, 2, .., p \quad \text{when} \quad i \neq j, \\
\boldsymbol{\mathcal{R}}_{3,i}^{(l)} &= \mathbf{R}_{3,i}^{(l)} - \left(\boldsymbol{\beta}_r^{(l)} d_{i,N_\zeta} \mathbf{I} + \boldsymbol{\gamma}_r^{(3,l)} d_{i,N_\zeta} \mathbf{D} \right) \mathbf{F}_{3,N_\zeta}^{(l)} \quad \text{word or phrase} \quad i = 0, 1, 2, ..., N_\zeta,
\end{aligned}$$

$\mathbf{I}$ is an $N_\eta(N_\zeta + 1) \times N_\eta(N_\zeta + 1)$ identity matrix.

The systems of matrix equations obtained in the first and second numerical experiments are then solved in `GNU Octave`. In the following chapter, we present the results that we got.

4. Results and Discussions

In this essay, the system of equations (3.1.5) and (3.2.8) have been solved using the multi-domain bivariate spectral local linearization method (MD-BSLLM) which was described in chapter 2. The MD-BSLLM was implemented in `GNU Octave`. In this section, we give the full analysis of the experimental results, and also make a comparison of the numerical results we obtained from the MD-BSLLM with literature values from the bivariate spectral local linearization method [22]. We further present a study of the significance of the system parameters on the fluid properties such as the skin friction, Nusselt number and Sherwood number.

4.1 Results and Discussions from Numerical Experiment 1

In the first numerical experiment, we solved the steady free convective flow of a fluid past a non-isothermal vertical porous cone. The computational domain extent of $\eta_\infty = 20$ was chosen in the η-direction. The number of sub-intervals q in the η-direction was maintained at 40 and the number of Chebyshev-Gauss-Lobatto grid points was chosen to be 5 in the ζ direction throughout the numerical experiment.

4.1.1 Parameter Profiles Analysis. Figure 4.1 below displays the velocity and the temperature profiles of the fluid flow respectively. The parabolic nature of the velocity profile is in line with the one that was got by Hossain [18]. As the value of η increase, there is a corresponding increase in the velocity at lower values of η and at values of $\eta > 1$, we see a decrease in the velocity of the fluid as shown in Figure 4.1a. Figure 4.1b shows that an increase in the value of η will result to an exponential decrease in the temperature. As the value of ζ increases, we can see a corresponding increase in the velocity and temperature profiles.

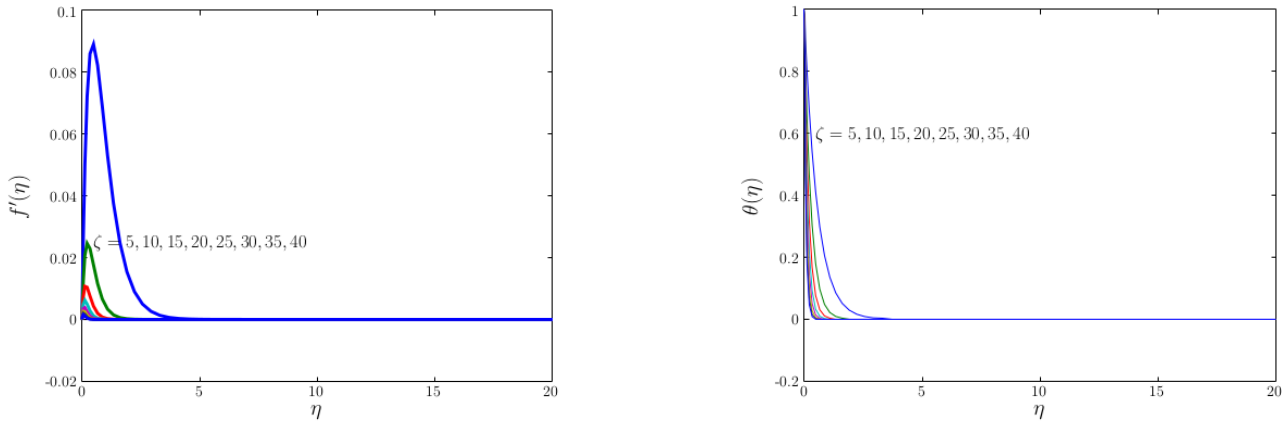

(a) Velocity profile

(b) Temperature profile

Figure 4.1: Profiles at different values of $\zeta = 5, 10, 15, 20, 25, 30, 35, 40$, $n = 0.5$, $w = 0.5$, $Pr = 0.7$, $Sc = 0.6$.

4.1.2 Convergence Analysis. We analyzed the convergence of the method by plotting the errors we got from the numerical method against the number of iterations. We define the errors as the difference between the approximate values of the functions at two successive iterations. Figure 4.2 below5 presents

the convergence of the numerical method, and the infinity norm was used to show the convergence. The infinity norm was defined by

$$E_W = \lim \max_{0 \geq i \geq N_\eta} ||W_{r+1,i} - W_{r,i}||_\infty \quad \text{for} \quad W = f, \theta, g, h. \tag{4.1.1}$$

From the graphs 4.2a and 4.2b below, it can be observed that the MD-BSLLM converge after 5 iterations and this suggest that the MD-BSLLM is convergent.

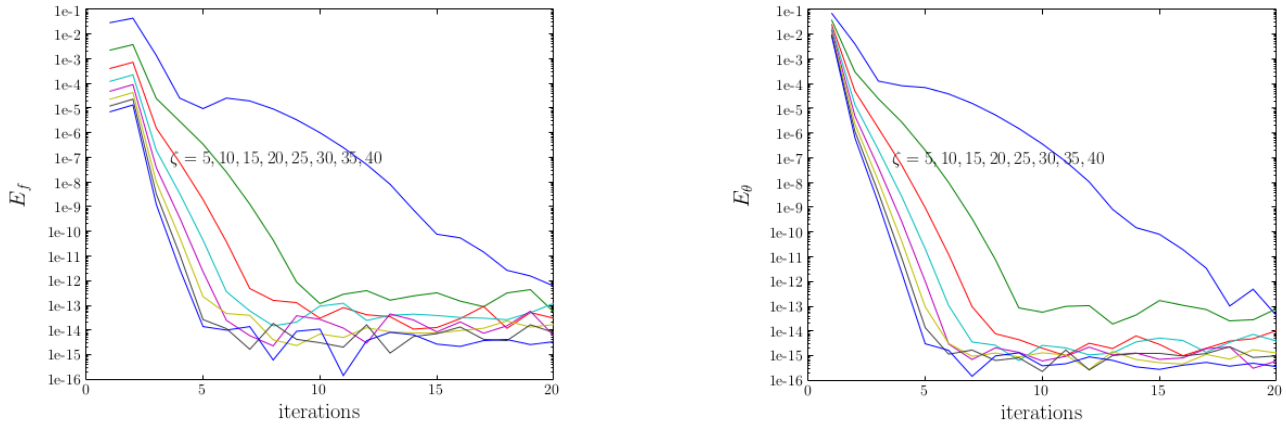

(a) (b)

Figure 4.2: Convergence graphs at different values of $\zeta = 5, 10, 15, 20, 25, 30, 35, 40$, $n = 0.5$, $w = 0.5$, $Pr = 0.7$, $Sc = 0.6$.

4.1.3 Accuracy Analysis. Figure 4.3 below shows the graphs of the residuals plotted against the number of iterations, with increasing value of ζ. From the graphs, we observe that the residual errors are not higher than 10^{-7} even from the first iteration. This reflects the accuracy of the MD-BSLLM.

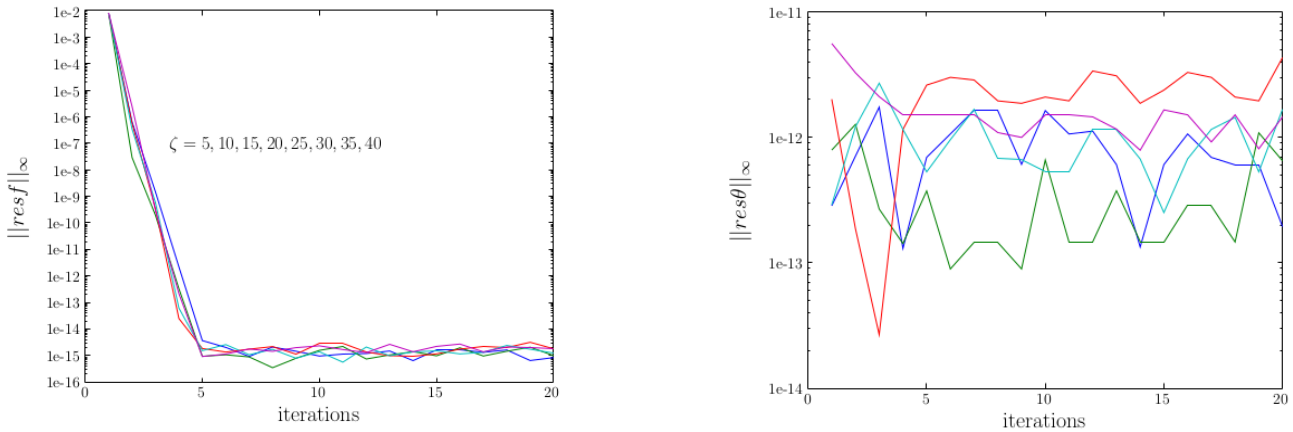

(a) (b)

Figure 4.3: Residual graphs at different values of $\zeta = 5, 10, 15, 20, 25, 30, 35, 40$, $n = 0.5$, $w = 0.5$, $Pr = 0.7$, $Sc = 0.6$.

4.2 Results and Discussions from Numerical Experiment 2

In the second experiment, we solved the steady convective flow of a viscous incompressible fluid along a permeable vertical flat surface using the MD-BSLLM. The computational domain extent of $\eta_\infty = 20$ was chosen in the η-direction. The number of sub-intervals q in the η-direction was maintained at 40 and the number of Chebyshev-Gauss-Lobatto grid points was chosen to be 5 in the ζ-direction throughout the numerical experiment.

4.2.1 Convergence Analysis. We analyzed the convergence of the method by plotting the errors we got from the MD-BSLLM against the number of iterations. We define the errors as the difference between the approximate values of the functions at two successive iterations. Figure 4.4 below presents the convergence of the numerical method, and the infinity norm as defined in (4.1.1) was used to show the convergence of the method. In Figure 4.4, we see that the method converges after 5 iterations. As the number of iterations increases, we can observe a decrease in the error norm and this suggests that the method is convergent.

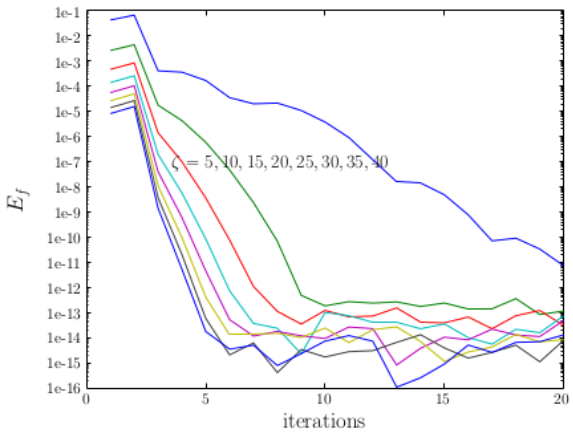

(a)

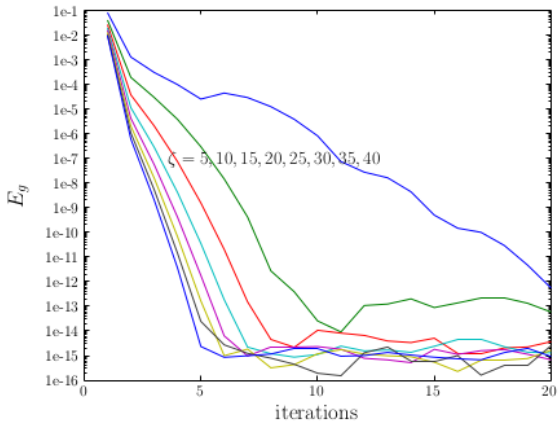

(b)

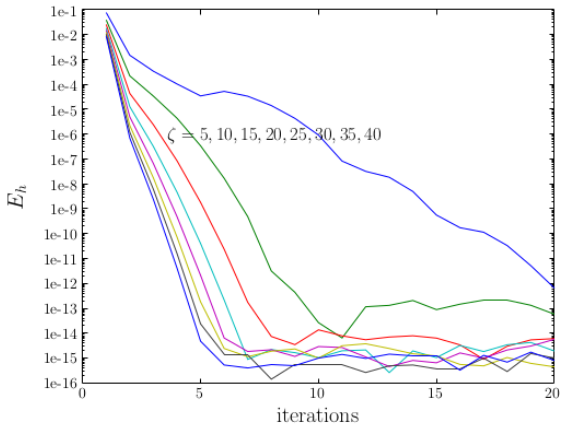

(c)

Figure 4.4: Convergence graphs at different values of $\zeta = 5, 10, 15, 20, 25, 30, 35, 40$, $n = 0.5$, $w = 0.5$, $Pr = 0.7$, $Sc = 0.6$.

4.2.2 Accuracy Analysis. The accuracy of the method solution was determined using the residual errors of the functions after a specific number of iterations. The approximate solution was substituted into (3.2.8) and the infinity norm was determined. In Figure 4.5, the graphs show the variation of the residual error against the number of iterations and we can observe that as the number of iterations increase, the residuals decrease. In all the graphs, the residuals remain less than 10^{-11}. This level of accuracy in the solutions $f(\zeta,\eta), g(\zeta,\eta)$ and $h(\zeta,\eta)$ was obtained in the second iteration. This reflects the accuracy of the MD-BSLLM.

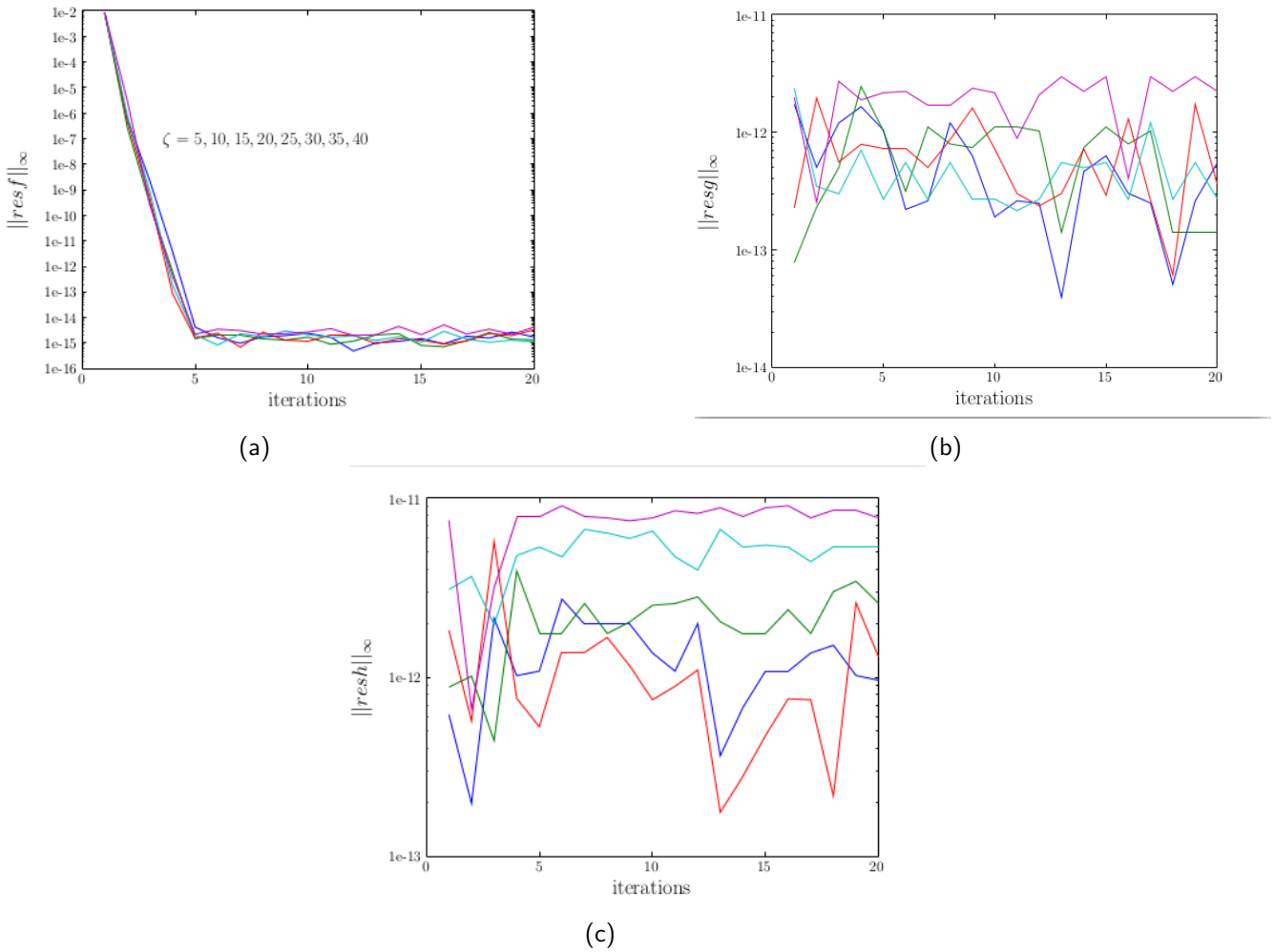

(a) (b)

(c)

Figure 4.5: Residual graphs at different values of $\zeta = 5, 10, 15, 20, 25, 30, 35, 40$, $n = 0.5$, $w = 0.5$, $Pr = 0.7$, $Sc = 0.6$.

4.2.3 Parameter Profiles Analysis. The graphs in Figure 4.6 below present the velocity, temperature and concentration profiles respectively for different values of η. In 4.6a below, we observe that an increase in η leads to an increase in the velocity for small values of $\eta < 1$ and for values of $\eta > 1$ we see a decrease in the velocity of the fluid as you increase η. The velocity profile of the fluid is a parabola, which is in line with what Hossain [18] got. In 4.6b and 4.6c both profiles show an exponential decay when you increase η which is also in agreement with what other researchers have got. These results validate the numerical method used in this study.

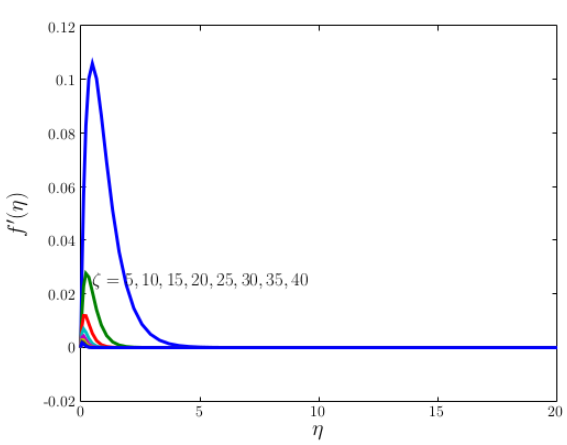

(a) Velocity profile

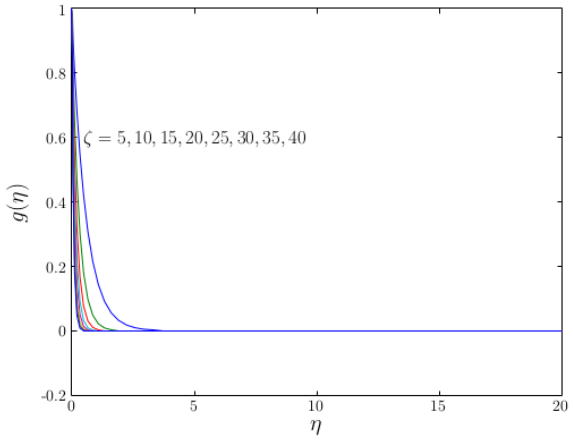

(b) Temperature profile

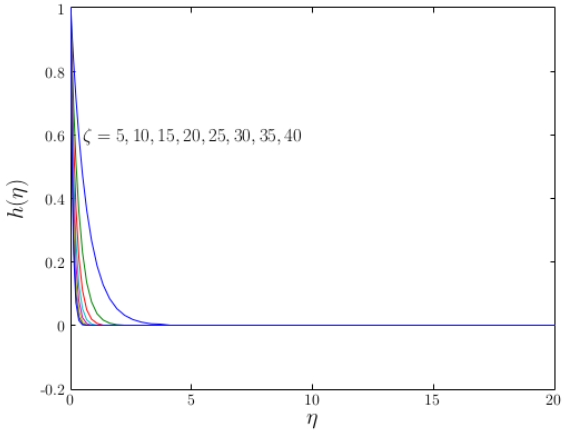

(c) Concentration profile

Figure 4.6: Profiles at different values of $\zeta = 5, 10, 15, 20, 25, 30, 35, 40$, $n = 0.5$, $w = 0.5$, $Pr = 0.7$, $Sc = 0.6$.

In the following subsection, we compare the solutions (at selected grid points) obtained by solving the steady convective flow of a viscous incompressible fluid along a permeable vertical flat surface model equations using the MD-BSLLM with the series solution method and also the bivariate local linearization method (BSLLM). Deductions are made based on the differences of the results and also on the computational costs.

4.2.4 Comparison of Results from MD-SLLM and BSLLM. In Table 4.1 below, we compare the solutions of the second system of equations obtained from the BSLLM and the MD-BSLLM. We observe that the solutions are almost the same, that is, there is no significant difference between the results, but there is a significant difference between the computational time. The MD-BSLLM takes about 20 seconds to achieve accurate results while the BSLLM takes about 80 seconds to achieve accurate results on the same domain. This marks the superiority of the MD-BSLLM over the BSLLM in terms of computational cost.

	BSLLM			Multi-Domain BSLLM		
ζ	$f''(0,\zeta)$	$-g'(0,\zeta)$	$-h'(0,\zeta)$	$f''(0,\zeta)$	$-g'(0,\zeta)$	$-h'(0,\zeta)$
5	0.3088066	3.5018993	3.0018843	0.3088214	3.5018961	3.0018658
10	0.1547399	7.0002370	6.0002332	0.1547399	7.0002370	6.0002332
15	0.1031717	10.500702	9.0000691	0.1031717	10.5000702	9.0000691
20	0.0773801	14.0000296	12.0000292	0.0773803	14.0000296	12.0000292
CPU Time	77.921	77.921	77.921	19.693	19.693	19.693

Table 4.1: Comparison of the MD-BSLLM and the BSLLM solution for $f''(0,\zeta)$, $-g'(0,\zeta)$ and $-h'(0,\zeta)$: $N_\eta = 60$, $N_\zeta = 5$, $n = w = \frac{1}{2}$, $Pr = 0.7$, $Sc = 0.6$, $q = 40$

5. Conclusion and Recommendations

5.1 Conclusion

In this essay, we were able to solve the two distinct boundary layer equations that model the steady free convective flow of a fluid past a non-isothermal vertical porous cone and the steady free convective flow of a viscous incompressible fluid along a permeable vertical flat surface. The main purpose of this study was to establish the applicability of the multi-domain bivariate spectral local linearization method and the feature that makes it computationally efficient than the bivariate spectral local linearization method. The results obtained in this study provide evidence that the method can be used to solve boundary layer flows and also for validating other numerical methods invented to solve non-similar boundary layer equations.

5.2 Recommendations

For future research purposes, the method can be extended to solve other model equations that arise in fluid mechanics such as unsteady boundary layer flow problems. Moreover, the Chebyshev interpolating polynomials can also be used instead of the Lagrange interpolating polynomial for the construction of the assumed solution in order to achieve high accuracy of the method.

Acknowledgements

I would like to thank the African Institute for Mathematical Sciences for giving me the opportunity to be part of the 2017/2018 cohort and do research on partial differential equations.

References

[1] Abbasbandy, S. (2008). Approximate solution for the nonlinear model of diffusion and reaction in porous catalysts by means of the homotopy analysis method. *Chemical Engineering Journal*, 136(2-3):144–150.

[2] Al-Shibani, F., Ismail, A. M., and Abdullah, F. (2012). The implicit keller box method for the one dimensional time fractional diffusion equation. *Journal of Applied Mathematics and Bioinformatics*, 2(3):69.

[3] Bachok, N., Ishak, A., and Pop, I. (2012). Unsteady boundary-layer flow and heat transfer of a nanofluid over a permeable stretching/shrinking sheet. *International Journal of Heat and Mass Transfer*, 55(7-8):2102–2109.

[4] Bader, G. (2018). Introduction to scientific computing with python.

[5] Batchelor, G. K. (2000). *An introduction to fluid dynamics*. Cambridge university press.

[6] Bender, C. M. and Orszag, S. A. (1999). Advanced mathematical methods for scientists and engineers. i. asymptotic methods and perturbation theory. reprint of the 1978 original.

[7] Cengel, Y. A., Pérez, H., et al. (2004). Heat transfer: a practical approach. transferencia de calor.

[8] Cheng, C.-Y. (2015). Free convection heat transfer from a non-isothermal permeable cone with suction and temperature-dependent viscosity. 18(1):17–24.

[9] Chhabra, R. P. and Richardson, J. F. (1999). *Non-Newtonian Flow: Fundamentals and Engineering Applications*. Butterworth-Heinemann.

[10] Davis, P. J. (1975). *Interpolation and approximation*. Courier Corporation.

[11] Evans, L. C. (1997). *Partial Differential Equations*. American Mathematical Society.

[12] Faires, D, B. L. (2010). *Numerical Analysis*. Brooks/Cole CENGAGE learning.

[13] Gottlieb, D. and Orszag, S. (2007). Spectral methods: Evolution to complex geometries and applications to fluid dynamics.

[14] Guo, W., Labrosse, G., and Narayanan, R. (2013). *The application of the Chebyshev-Spectral method in transport phenomena*. Springer Science & Business Media.

[15] He, J.-H. (1999). Variational iteration method–a kind of non-linear analytical technique: some examples. *International journal of non-linear mechanics*, 34(4):699–708.

[16] He, J.-H. (2003). Homotopy perturbation method: a new nonlinear analytical technique. *Applied Mathematics and computation*, 135(1):73–79.

[17] Hossain, M. and Paul, S. (2001). Free convection from a vertical permeable circular cone with non-uniform surface temperature. *Acta Mechanica*, 151(1-2):103–114.

[18] Hussain, S., Hossain, M., and Wilson, M. (2000a). Natural convection flow from a vertical permeable flat plate with variable surface temperature and species concentration. *Engineering Computations*, 17(7):789–812.

[19] Hussain, S., Hossain, M., and Wilson, M. (2000b). Natural convection flow from a vertical permeable flat plate with variable surface temperature and species concentration. *Engineering Computations*, 17(7):789–812.

[20] Liao, S. (2003). *Beyond perturbation: introduction to the homotopy analysis method*. CRC press.

[21] Magagula, V., Motsa, S., and Sibanda, P. (2017). A multi-domain bivariate pseudospectral method for evolution equations. *International Journal of Computational Methods*, 14(04):1750041.

[22] Magagula, V. M. (2016). On the multi-domain bivariate spectral local linearisation method for solving system of non-similar boundary layer equations. In *Conference Abstracts*, volume 1.

[23] Magagula, V. M., Motsa, S. S., Sibanda, P., and Dlamini, P. G. (2016). On a bivariate spectral relaxation method for unsteady magneto-hydrodynamic flow in porous media. *SpringerPlus*, 5(1):455.

[24] Motsa, S. (2014). On the bivariate spectral homotopy analysis method approach for solving nonlinear evolution partial differential equations. In *Abstract and Applied Analysis*, volume 2014. Hindawi.

[25] Motsa, S. (2015). On the new bivariate local linearisation method for solving coupled partial differential equations in some applications of unsteady fluid flows with heat and mass transfer. In *Mass Transfer-Advancement in Process Modelling*. InTech.

[26] Motsa, S. (2017). Numerical analysis lecture notes.

[27] Motsa, S. S. (2013). A new spectral local linearization method for nonlinear boundary layer flow problems. *Journal of Applied Mathematics*, 2013.

[28] Motsa, S. S., Dlamini, P. G., and Khumalo, M. (2014). Spectral relaxation method and spectral quasilinearization method for solving unsteady boundary layer flow problems. *Advances in Mathematical Physics*, 2014.

[29] Otegbeye, O. (2014). On decoupled quasi-linearization methods for solving systems of nonlinear boundary value problems.

[30] Paterson, W. and Hayhurst, A. (2000). Mass or heat transfer from a sphere to a flowing fluid. *Chemical Engineering Science*, 55(10):1925–1927.

[31] Perot, J. B. and Subramanian, V. (2007). A discrete calculus analysis of the keller box scheme and a generalization of the method to arbitrary meshes. *Journal of Computational Physics*, 226(1):494–508.

[32] Pruett, C. D. and Streett, C. L. (1991). A spectral collocation method for compressible, non-similar boundary layers. *International journal for numerical methods in fluids*, 13(6):713–737.

[33] Sajid, M. and Hayat, T. (2007). Non-similar series solution for boundary layer flow of a third-order fluid over a stretching sheet. *Applied mathematics and computation*, 189(2):1576–1585.

[34] Sanders, C. and Holman, J. (1972). Franz grashof and the grashof number. *International Journal of Heat and Mass Transfer*, 15(3):562–563.

[35] Satsuma, J., Ablowitz, M., Fuchssteiner, B., and Kruskal, M. (1987). Topics in soliton theory and exactly solvable nonlinear equations. *World Scientific, Singapore City*.

[36] Trefethen, L. N. (2000). *Spectral methods in MATLAB*, volume 10. Siam.

[37] Vajravelu, K. and Van Gorder, R. (2013). *Nonlinear flow phenomena and homotopy analysis*. Springer.